University of Alberta

Weather-based Thermal Rating of Overhead Power Transmission Lines

by

Konstantin Filimonenkov

A thesis submitted to the Faculty of Graduate Studies and Research
in partial fulfillment of the requirements for the degree of

Master of Science

in

Software Engineering and Intelligent Systems

Department of Electrical and Computer Engineering

Fall 2011
Edmonton, Alberta

Abstract

One of the ways to improve electric power transmission systems is to efficiently utilize the capacity of the existing power circuits. That can be achieved by increasing the thermal ratings of the transmission lines. In this research, weather-based rating approaches were studied. Static thermal rating (STR) strategies (probabilistic and seasonal) and a new dynamic thermal rating (DTR) approach based on numerical weather prediction (NWP) were evaluated. The results demonstrate that the DTR approach allows better line utilization compared to STR methods. It was also shown that the postprocessing technique called model output statistics (MOS) can significantly reduce errors in numerical weather simulation, improve the accuracy of the DTR system, and reduce the risks of line overheating. Efficient data management, processing, and visualization were investigated to fully utilize the potential of an advanced DTR system. Applications of the latest web-based technologies, geospatial databases, and 3D visualization techniques are presented.

Acknowledgements

I thank my supervisor Dr. Petr Musilek for giving me an incredible opportunity to study at the University of Alberta and to be part of his research group. Thanks to his initiative, guidance, and support, I was able to obtain very valuable knowledge and experience and advance my career path.

I thank all the members of the group for their valuable contributions and assistance. It was a pleasure to study and work with smart, dedicated specialists. I hope we will find a way to keep in touch.

Finally, I thank my parents who were far from me during the years in graduate training, but who always understood, encouraged, and supported my desire to pursue an MSc degree at the University of Alberta.

Contents

List of Figures

Figure

List of Tables

Table

Chapter 1

Introduction

1.1 Motivation

The capacity of current high-voltage electric transmission systems must be increased to meet the growing power demand and to support development of clean generating stations that work with renewable sources of energy. The annual report prepared by the International Energy Agency, World Energy Outlook 2010, predicts the worldwide demand for electric energy will continue to grow at a rate higher than any other final form of energy. Between 2008 and 2035 the demand for electricity will rise by 2.2 % per year. As an example, in the 15 years after 2010, China is planning to install additional generation capacity equal to the current generation capacity of the United States. Worldwide, between 2009 and 2035, gross capacity additions will reach 5,900 gigawatts (GW), which is 25 % more than the present installed capacity. It is projected that more than 40 % of these additions will be accomplished by 2020 [2].

Another important trend in the power industry today is providing clean power by leveraging renewable sources of energy such as solar radiation, wind, and geothermal heat. Electric power generating stations that use renewable sources of energy may not be located close to a main backbone of high-voltage transmission

circuits with high transmission capacity, and the generated energy must be transmitted through the existing lines in the area. Such lines usually have low carrying capacity, and at times of increased load they can be significantly stressed [3].

To cope with increased energy demands and to support clean energy initiatives, the capacity of transmission systems must be increased. The straightforward solution is to build new transmission circuits. However, this approach is costly and it can take several years before a new line is ready for use. Major obstacles to building new transmission circuits are obtaining right-of-ways (ROW) for the new lines, meeting governmental and environmental regulations, and persuading people from the communities near the proposed transmission corridors to allow construction. Therefore, companies are looking for ways to increase the capacity of existing transmission lines [4].

Power carrying capacity of transmission systems can be increased if energy is transmitted more efficiently. The maximum current-carrying capacity of a transmission circuit can be estimated by the maximum electric power that can be transmitted by a line

$$capacity = P = I \times V \tag{1.1}$$

where I is the maximum allowable electric current, and V is the voltage of the transmission line. Equation (1.1) shows that to increase the capacity of the line, I and/or V must be increased. Higher voltage and/or higher electric current will deliver higher electric power and therefore more energy will be transmitted over the line.

However, the designed line voltage is not easily increased. Voltage uprating requires that the entire circuit be reconstructed; insulators must be replaced, transmission structures must be raised, and space between the conductors must be increased, among other things, yielding a cost as high as the cost of building a new transmission line [5].

A better solution is to increase the maximum electric current in the line. Current uprating can be accomplished without modifying power lines. However, this procedure must be performed cautiously, as a higher electric current might violate the thermal limit (the maximum safe temperature) of the conductor.

A conductor thermal limit is a constant value (usually $75 - 125\,^{\circ}\mathrm{C}$) that depends on the physical characteristics of the conductor material and the safety requirements of the circuit. The actual temperature of the conductor varies spatially and temporally; it depends on factors that are constantly changing, like the magnitude of the electric current and ambient weather conditions along the line [6]. Weather parameters such as wind, air temperature, solar radiation, and precipitation can significantly influence conductor temperature (either cool it down or heat it up) [7]. Assuming that the electric current remains constant, the conductor temperature will change spatially and temporally, as the weather conditions change along the transmission circuit and in time. Therefore, identifying the conductor temperature at each line span, or the line ampacity (the maximum safe electric current), requires knowing the weather conditions along the line. Currently, this challenging problem does not have a cost-effective and reliable solution [8].

To determine the maximum electric current that can be safely carried by a transmission line, electric utilities most frequently use a deterministic static thermal rating approach based on assumptions of constant unfavourable weather conditions along the circuit [9] [10]. A thermal rating value (the maximum allowable electric current) is chosen that will ensure the risk of violating the line thermal limit is relatively low. To estimate the static thermal rating for the line, the air temperature is usually assumed to be $30\,^{\circ}\mathrm{C}$ and the wind speed to be $2\,\mathrm{m/s}$. Most of the time transmission lines will be operated under more favourable weather conditions (lower ambient temperature, higher wind speed), and the thermal rating will be less than the actual line ampacity [11]. This leads to underutilization of transmission circuits, as the potential current-carrying capacity of the lines is not

fully utilised. At the same time, the conservative weather parameters are not the worst possible cases, and the thermal limit can still be violated at times of worse weather conditions [12]. Therefore, advanced methods of thermal rating are needed to increase transmission system capacity while preserving reliability and safety.

1.2 Thesis objectives

The main goal of the research described in the thesis is to investigate three weather-based thermal rating approaches: seasonal static rating, static rating based on data for a typical meteorological year, and dynamic thermal rating (DTR) based on numerical weather simulations. This study includes (i) assessment of how much the capacity of transmission lines can be increased by applying probabilistic static thermal rating approaches or by a dynamic thermal rating approach based on numerical weather prediction, (ii) estimation of the risks of line overheating depending on a chosen rating strategy, (iii) application of model output statistics to the improvement of DTR calculation accuracy, and (iv) a review of important practical aspects of building an advanced DTR system for transmission system operation.

Seasonal rating is a set of several static thermal ratings statistically determined for various time intervals. By alternating among several such ratings, it is theoretically possible to operate the line closer to its actual ampacity. However, their use may increase the risk of line overheating.

A static thermal rating based on data for a typical meteorological year is another probabilistic rating commonly used as an alternative to a deterministic thermal rating. It is usually higher than the deterministic rating allowing better utilization of potential line capacity. However, similar to the seasonal static rating, the risk of line overheating may increase.

The third rating evaluated in this thesis is dynamic thermal rating based

on numerical weather prediction (NWP). DTR is a method of controlling the line ampacity in real time by accounting for actual weather conditions along the circuit. Existing DTR systems [13] [14] [15] [16] determine ampacity only at a few locations along a line. NWP provides data with high spatial resolution that allows the rating to be calculated at each conductor span along the entire line.

At the same time, uncertainty of NWP results may introduce errors in DTR calculations. To reduce these errors and increase the accuracy of the dynamic thermal rating, a technique called model output statistics is applied. The objective of this study is to assess improvements in the accuracy of the thermal rating provided by an NWP-based DTR system.

To implement and efficiently utilize an NWP-based DTR system, modern information technologies must be applied. The last part of this thesis focuses on data management and data visualization for the advanced DTR system; aspects of efficient data analysis, data storage, and data visualization are evaluated. The objectives include application of Web-based interactive graphics and plots, as well as design and implementation of an advanced 3D visualization system for transmission system operation.

1.3 Thesis organization

The thesis is organized in six chapters. The literature on thermal rating strategies is reviewed in chapter 2. Chapter 3 presents concepts of thermal rating (section 3.1), seasonal static rating and static rating based on data for a typical meteorological year (TMY) (section 3.2), and dynamic thermal rating based on numerical weather simulations (section 3.3). Two case studies evaluating various rating approaches (seasonal rating, TMY rating, NWP-DTR) at two different locations – a test site in British Columbia and a test site in Newfoundland and Labrador – are also presented in chapter 3 (subsections 3.2.1.1 and 3.2.2.1).

Chapter 4 describes a way to enhance the NWP-based DTR approach by improving the accuracy of numerical weather simulations using model output statistics (MOS). The theoretical background of MOS algorithms (sections 4.1, 4.2, and 4.3) is presented and a methodology for MOS application in the DTR-NWP system (section 4.4) is provided. The MOS technique is evaluated in a case study (section 4.5). The results demonstrate a significant reduction in weather parameter errors and in the errors in the thermal rating that is calculated based on numerical weather simulation data.

Chapter 5 reviews aspects of building an advanced NWP-based DTR system and integrating it into the operation of a transmission system, including data organization, data processing, and data visualization for the DTR. The first section covers database organization for storing numerical weather simulations and geospatial characteristics of transmission system assets. In section 5.2, Web-based graphics and plots are discussed. Several examples of geospatial visualization and interactive graphics of weather conditions and ampacity calculations are presented. The last section presents a 3D visualization system of transmission system assets, which can be used not only for the needs of the DTR system but also for asset management, system planning and operation, and new line design.

Chapter 5 is followed by a conclusion where research outcome, achievements, and future directions are summarized.

Chapter 2

Literature Review

A number of publications on the topic of thermal rating are reviewed in this chapter. The condensed summary of published works presented in this chapter helped to build a theoretical background in the research area and acquaint the researcher with conventional terms and definitions. Research questions that have been comprehensively studied and questions that require further investigation were identified to justify the research objectives chosen for the project.

Early publications on the topic of thermal rating [17], [18], [19], [9] underline the importance of thermal rating for efficient transmission system operation and demonstrate that thermal rating must be based on real weather parameters to allow high transmission capacity. At the time of these publications, direct measurements of line tension, sag, and temperature were not possible.

[18] presents mathematical equations for calculating the maximum safe conductor current based on the assumed conductor temperature and weather parameters. The authors account for the effects of conductor surface conditions, wind velocity, altitude, and solar radiation on heat transfer. Later, [9] improves the equations provided in [18] by performing experiments on stranded conductors. The author establishes the heat balance equations for calculating the continuous rating of power lines having considered the effects of various atmospheric conditions.

Using equations in [18], [17] develops an approach to calculate transmission line thermal ratings based on historical weather conditions. The author uses the total loss of conductor strength due to annealing as the main limiting factor for thermal rating, and derives a new static rating based on the calculated loss of strength. The proposed method was an advanced alternative to the conventional thermal rating. The author demonstrates that the real ampacity is usually higher than the deterministic static rating, and the line rating can be increased. At the same time, dynamic real-time thermal (or "continuous," the term used by the author) rating is stated as being unrealistic. At that time it was not feasible to dynamically monitor line rating. [19] further develops an idea of dynamic thermal rating by modeling weather parameters.

[19] builds a weather model based upon actual weather observations and applies Pearson's model of moments to generate curves of possible conductor temperatures. This may be considered as the first attempt to calculate real-time conductor temperature by modeling weather parameters. However, in both [17] and [19], wind direction is still assumed to be perpendicular to the conductor, and the effects of different wind directions are not considered. In [20], for the first time, it is shown that the conductor temperature depends highly on the azimuth of the transmission line (or wind incidence to the conductor).

Five articles [7], [21], [22], [20], [23] present well-organized, detailed, and comprehensive research on dynamic thermal rating. The significant and valuable research performed by Davis was originally slated to be published in nine articles; only five of the planned papers were eventually written.

Based on historical weather data, [7] shows the benefits of dynamic thermal rating and proposes a "real time thermal rating system" intended to monitor thermal rating in real time and predict characteristics such as loss of conductor strength and sag using weather models. In the next three articles [21], [22], [20], the author analyzes the impact of weather parameters on conductor temperature

and covers topics such as forced and natural convection, total solar radiation (including beamed and diffuse radiation), atmosphere attenuation, and correlations of weather parameters in time. In the latest paper [23], the author thoroughly investigates the impact of wind velocity and wind direction on thermal rating. It is shown that the conventional static rating can violate the thermal limit of the conductor up to 9 % of the time, which is much higher than the risk usually associated with the conventional static rating (0.02 %). Such a significant discrepancy is explained by the fact that the deterministic rating is calculated assuming a wind direction perpendicular to the conductor. For example, a wind speed of 3.2 m/s, which is twice as high as the assumed conservative wind speed, can increase conductor temperature to 16 % higher than the thermal limit (100 °C) if the wind blows parallel to the conductor.

Three years later, two companion papers [24], [25] presented an important experimental verification of the dynamic real-time thermal rating algorithms [18]. At the outdoor test site designed specifically for this research, the temperature of the conductor was measured directly by thirteen thermocouples installed along the line span. The temperature was also calculated with the computer program [24]. Real-time weather data, needed for deriving conductor temperature, were obtained from weather stations mounted in the immediate vicinity of the mid-span. The calculated and measured temperatures were then compared. A few important observations were outlined in the paper: (1) the conductor temperature varied significantly along a single span (up to 10 °C), (2) the conductor temperature calculated based on the weather data was within 10 °C of the average measured temperature, and (3) the two most important weather parameters affecting conductor temperature were wind speed and wind direction. The authors demonstrate that the real-time ampacity of a single span can be estimated with fair accuracy based on just three weather parameters: wind velocity, wind direction, and ambient temperature. The authors also emphasize that the conductor temperature

varies significantly along the line depending on local weather patterns. Thus, a single weather station may be insufficient to accurately monitor line ampacity. Similar results were obtained from the experimental evaluation of DTR algorithms presented in [26],[27]

Concerns that there are differences between dynamic thermal ratings of a single span and an entire line are further explored in [10] and [28]; the former is a comprehensive summary of up to date research achievements in the area of dynamic thermal rating. One of the essential unresolved problems mentioned in the paper is the calculation of the thermal rating for a whole transmission line, not just for a single span. Three main obstacles for calculating the thermal rating of an entire line were underlined in the paper: (1) variation of wind speed and wind direction along the line, (2) variation in the line spans' azimuths, and (3) the sheltering effect of vegetation and terrain.

[28] also points out that a distinction between the DTR for a single span and the DTR for an entire line must be made in order to more realistically estimate line ampacity. The author calculates thermal rating by considering historical weather observations and different directions of the line span in question. It is concluded that if the line had spans in all possible directions, there would always be a span that was parallel to the wind. As a result, the line must be rated assuming a parallel wind instead of the perpendicular wind that is used to establish the deterministic static rating.

[28] also mentions the importance of the prediction of line ampacity in the future; it is essential for a transmission system operator to know how much the line rating can change over time. The author proposes an approach of predicting the minimum thermal rating up to $1 - 4$ hours ahead, based on the statistical analysis of historical weather data. However, in the discussion section of the paper, such an approach is criticized as excessively conservative as it does not consider the time correlation between weather parameters and load patterns. [29] presents a more

advanced method of forecasting thermal rating, which allows an increase in the average power flow on a line.

Practical limitations on the use of dynamic thermal rating presented in [28] were further studied on a short transmission line in the area of Rochester, NY [30]. The main focus of the case study was to investigate the critical span distribution and to check if the dynamic thermal rating, calculated using weather data from a single weather station, can be expanded for an entire line. The results show that the line hot spots change over time according to local weather patterns. The authors also conclude that remote weather stations, located as far as 30 km away from the transmission line, can potentially be used for DTR, but in this case, all possible span orientations of the line must be accounted for.

More conservative conclusions are made in [31]. This paper, similar to [30], presents the results of research focused on the identification of a critical line span. The authors emphasize that locations of critical line spans are difficult to determine due to the high variability of local weather conditions. It is shown that the number of hot spots and their locations change in time, and that conductor temperature varies significantly along the circuit.

More recent publications on the topic of dynamic thermal rating [11], [32], [3] , [33], [6] describe the benefits of DTR using results of case studies involving line spans. The fact that the dynamic rating of the line span is not the same as the rating of the entire line is a problem that is not solved in the published research. The available commercial DTR systems – ThermalRate [13], Sagometer [14], tension-based system [15] – can calculate ampacities with fairly high accuracy, but only for line spans where they are installed.

[1] presents a new advanced DTR system based on the numerical weather prediction (NWP) model. Weather prediction of high temporal and spatial resolutions from the weather research and forecasting (WRF) model is used to calculate ampacities of each span of a transmission line and estimate the thermal rating for

the line based on the lowest ampacity along the line. Such a system possesses obvious advantages over other dynamic thermal rating approaches as it can provide an accurate rating for the whole line, not just a span rating.

Chapter 3

Thermal Rating

3.1 Main concepts and definitions

3.1.1 Thermal limit

The temperature of a high-voltage overhead transmission line conductor must be always below its thermal limit – the maximum allowable temperature. The sag of a conductor between towers increases as its temperature increases. When the temperature is too high (typically more than $75-120\,^{\circ}\mathrm{C}$), a violation of prescribed conductor-to-ground clearance can occur, which can cause severe safety and reliability risks. Also, high conductor temperatures change physical characteristics of the conductor material – an annealing process wherein the conductor cannot shrink back to its original length when cooled. As the sag increases, and the overall reliability of the transmission system decreases due to loss of tensile strength of the overheated conductor. In addition, when a conductor is overheated, power transmission becomes less efficient [34].

Conductor temperature is a function of various parameters, the complete list of which may be found in [9] and in [35]. The most significant influences are the electric current magnitude and its time duration, ambient weather conditions (temperature, wind velocity, precipitation, etc.), and conductor surface conditions

[36]. Line conductors are heated by electric current resistance and solar radiation. They are cooled by wind and by precipitation in the form of rain, dew, and snow.

3.1.2 Ampacity and thermal rating

Ampacity is the maximum amount of electric current a power line can carry before sustaining immediate or progressive deterioration; that is, ampacity is the maximum load the conductor can carry before exceeding its thermal limit. As weather parameters (e.g., wind velocity, ambient temperature) that influence conductor temperature are constantly changing, the ampacity of the line changes as well. Currently, there are no cost-effective, reliable methods to measure the conductor temperature along the entire line; thus, it is not possible for utilities to identify the line ampacity accurately [8].

The line thermal rating is the electrical current transmission companies use instead of actual ampacity to specify the maximum safe electric current that may be transferred through the circuit. The transmission capacity of the line increases as the current throughput increases. Therefore, an improvement in line rating accuracy could increase the line transmission capacity by allowing more current to flow through the line under favourable conditions. However, accurate line ratings are difficult to achieve due to lack of information about environmental conditions along the line.

3.1.3 Static thermal rating

To assure a low probability of violating the thermal limit, electric utilities often use a static thermal rating (STR) based on a conservative assumption of weather conditions [6]. The downside of such an approach is that the potential line loadability is significantly reduced [37]. Most of the time lines are operated under favourable weather conditions where they can be cooled by the wind and low ambient temperatures. When the line is cooled, the electrical current can be

increased without the risk of raising the conductor temperature above its thermal limit. An STR does not consider worst weather conditions wherein lines may be overheated. Thus, lines are underutilized and still exposed to risk of overheating during times of unfavourable weather. Dynamic thermal rating is a more energy efficient alternative.

3.1.4 Dynamic thermal rating

A dynamic thermal rating (DTR) defines the maximum safe electric current for a power line, accounting for the actual weather conditions along the transmission corridor. Dynamic ratings change over time due to changes in ambient weather patterns. The maximum current is relatively high during times of favourable weather conditions (high wind speed, low ambient temperature) and more energy can be safely transferred through the line. During adverse weather conditions (still wind, high air temperature) the dynamic rating is low (sometimes even lower than conventional static rating), and the conductor temperature never violates the thermal limit. Two advantages that make DTR preferable to STR are higher line electrical throughput and lower risk of line overheating.

3.1.5 Calculation of the current/temperature of bare overhead conductors

To calculate a lines thermal rating or a conductors temperature based on a specified electrical current and ambient weather conditions, utilities use industry standard IEEE-738 [35] or CIGRE W22 [38] These standards consider relationships among all major factors influencing the conductor temperature and provide formulas for the calculations. [39] showed that both methods produce similar results and can be considered equivalent for most practical applications. IEEE-738 was used in the current research for calculating ratings and line temperatures. IEEE-738

provides a numerical solution for the heat balance equation:

$$q_c + q_r = q_s + I^2 R(T_c), \tag{3.1}$$

where q_c is the heat loss rate due to convection, q_r is the heat loss rate due to radiation, q_s is the heat gain rate from the sun, and $I^2R(T_c)$ represents the Joule heating (also known as ohmic heating or resistive heating) of the conductor. By rearranging equation (3.1) it is possible to derive the thermal rating where electrical current I corresponds to a maximum permissible conductor temperature T_c.

$$I = \sqrt{\frac{q_c + q_r - q_s}{R(T_c)}}. \tag{3.2}$$

The parameters of equation (3.2) depend on conductor properties and ambient weather conditions. The conductor used for the research experiments was 795 Kcmil 26/7 ACSR Drake. It is a common type of conductor for overhead high-voltage transmission lines. The maximum allowable temperature of the Drake conductor is 75 °C for normal operation and 95 °C for short time emergencies. The coefficients of emissivity and absorptivity were assumed to be equal to 0.5. These values are usually used when the actual conditions of the conductor surface are unknown.

3.2 Static Thermal Rating (STR)

Currently, most utilities use static thermal ratings (STRs) to control the electric current in their transmission lines. Regardless of actual line ampacity, which is constantly changing due to changes in conductor temperature, the STR remains fixed. The STR is based on (1) assumptions of conservative ambient weather parameters recommended by regulatory agencies or conductor manufacturers – deterministic rating [9], [10], or (2) statistically determined unfavourable weather conditions in the area of the transmission line – probabilistic rating [28],

[17], [40] For both rating methods, the ambient weather conditions chosen must be rare occurrences, so that most of the time the lines are not overheated and the reliability of the transmission system is not endangered.

In many cases, electric utilities use the deterministic approach for calculating STR. This rating strategy is based on the assumptions that the weather conditions chosen for STR are highly unlikely and the temperature of the conductor will be below the thermal limit most of the time. Currently, industry standards do not outline what the rating conditions must be, and companies are free to choose weather parameters [6]. Typically, assumed ambient temperature is in the range of $30 - 40\,^{\circ}\mathrm{C}$, and wind speed is $0.61 - 1.53\,\mathrm{m/s}$ with a direction perpendicular to the conductor [10] Due to highly conservative weather parameters, thermal rating is far below actual line ampacity most of the time. High safety margins cause significant underutilization of the line, and the potential current carrying capacity idles. At the same time, while assumed weather conditions are rare occurrences, they are not worst case scenarios, and the temperature of the conductor can rise above the thermal limit when such events occur.

Probabilistic approaches to calculating thermal ratings are an advanced alternative to deterministic methods in that they aim to increase the throughput of the lines while preserving the safety and reliability of the transmission system. Probabilistic approaches utilize actual historical weather observations in the area of the transmission lines to establish rating conditions for calculating STRs [28]. The assumed weather parameters of the deterministic approach are usually more conservative than actual unfavourable weather conditions. By evaluating historical weather patterns, it is possible to statistically determine actual worst case weather parameters and apply them to STR calculations. Probabilistic ratings are typically higher than deterministic ones, thus, probabilistic ratings allow the capacity of the lines to be increased.

Probabilistic thermal rating can be calculated for different periods of time

(whole year, seasons, months, days, hours, etc.). Such an approach is called seasonal STR. By alternating among several probabilistic ratings according to the time intervals for which they were calculated, it is possible to operate the transmission line closer to its actual line ampacity. However, by increasing the capacity of the line, seasonal STR may increase the risks of line overheating. The assessment of seasonal STR is presented in section (3.2.1).

Another probabilistic approach evaluated in the thesis is STR based on weather data for a typical meteorological year (TMY). The historical weather data, processed and organized in a form of a TMY, usually consists of many years (several decades) of observations. This allows the resulting dataset to represent the typical weather parameters of the corresponding geographic area very well. The use of TMY weather data should allow more accurate estimation of the rating conditions, and thus a more accurate estimation of the STR for line operation. The study results of the probabilistic rating approach based on TMY weather data are presented in section (3.2.2).

3.2.1 Seasonal STR

Typically, electric utilities operate their transmission systems with two deterministic STRs estimated for two seasons of the yearwinter and summer. Weather assumptions for both ratings are usually same except for the ambient temperature. For instance, to establish a summer STR, BC Hydro utilizes air temperature equal to 30 °C, while 10 °C is assumed for calculating a winter STR. A wind speed of 0.6 m/s is used for calculating both summer and winter ratings [8]. In British Columbia, an ambient temperature of 30 °C during winter months is highly unlikely, and by reducing the weather parameter to the reasonable 10 °C, the electric utility can operate the line with a higher STR and thereby increase the capacity of the transmission system. The probabilistic seasonal STR approach is based on the same principle as the seasonal deterministic rating described above. However,

the probabilistic approach uses historical weather data to calculate ratings, and the amount of alternations during the year can be as high as 24 (individual ratings for 12 months and day/night time periods).

Probabilistic seasonal STR is expected to increase the current-carrying capacity of the system by allowing operation of the line closer to its actual ampacity, while preserving its safety and reliability. In the following case study the ampacity loss/gain of individual ratings is evaluated and the risks of line overheating under different rating strategies are compared.

3.2.1.1 Case study

Description of the Sample Power Transmission Line

The power transmission line TL201 operated by Newfoundland and Labrador Hydro was selected for this case study. The 230 kV-line is located in Newfoundland and connects the Hardwoods power plant and the Western Avalon substation. The first 200 towers of the line, starting from the Hardwoods substation, were considered in the study (Figure 3.1).

Historical weather observations are essential for calculating probabilistic thermal ratings. Using long periods of historical weather data, it is possible to identify the frequency of weather conditions that are critical for line operation, and then use the results to calculate a thermal rating. The North American Regional Reanalysis (NARR) historical weather dataset [41] was used to calculate probabilistic seasonal STRs. The weather data are provided on a regular grid of 32 x 32 km with a temporal resolution of 3 hours. Available weather parameters were fit to the locations of the transmission line towers by bicubic interpolation. Weather data were also interpolated in time from the original 3-hour to a final 1-hour resolution.

Ten years of NARR data (01/2000–12/2009) were divided into various time intervals for which seasonal ratings were determined. The classification of seasonal STRs considered in the case study is presented in Table 3.1. In the next step,

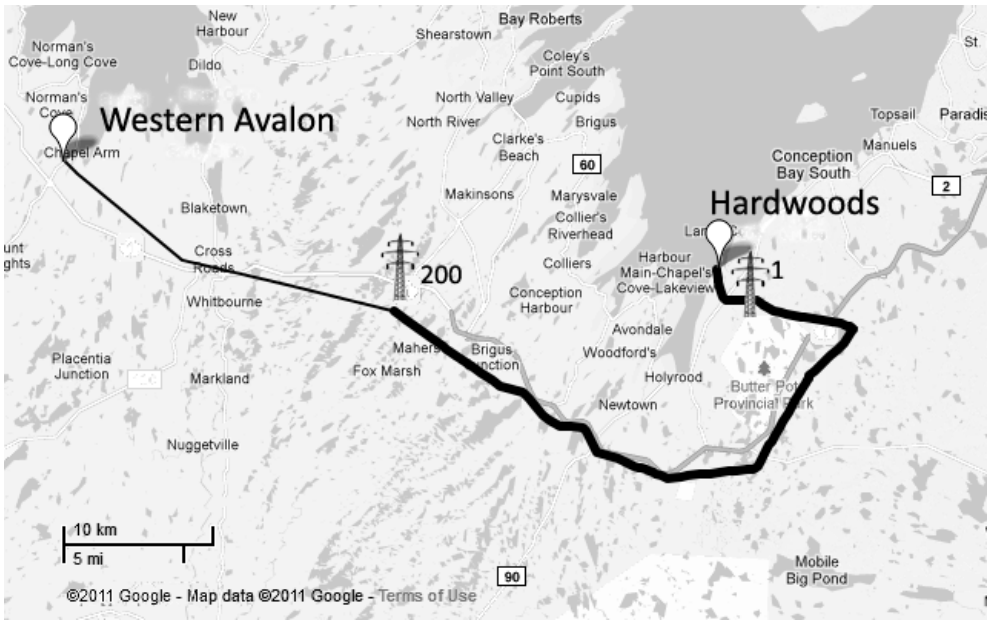

Figure 3.1: Location of power transmission line TL201 and two power stations (Western Avalon and Hardwoods).

STR Label	Amount of alterations per year	Description
STRa	1	Constant value of STR for whole year
STRb	2	Two seasons: Winter: November–April Summer: May–October
STRc	4	Four seasons Summer: June–August Fall: September–November Winter: December–February Spring: March–May
STRd	12	Twelve months
STRe	8	Four seasons and day-time (6am–6pm) night-time (6pm–6am)
STRf	24	Twelve months and day-time (6am–6pm) night-time (6pm–6am)

Table 3.1: Classification of Seasonal Static Thermal Ratings.

cumulative distribution functions (CDFs) were built for all values of air temperature and wind velocity for each time interval. The CDFs allow estimation of the

frequency of occurrence of weather parameters. The values of weather parameters corresponding to the quantiles of the CDFs may be interpreted as the weather parameters whose probability of occurrence is equal to the percentage of the quantile. For instance, if the 95 %-quantile of the CDF of ambient temperature is equal to 35 °C, it means that an air temperature of 35 °C or higher occurred 5 % of the time. The risk of thermal overload that an electric utility is willing to accept can be expressed as the probability of critical weather parameters, which in turn can be determined from the CDFs. The seasonal thermal rating can be calculated based on the determined critical weather conditions.

Estimation of Actual Transmission Capacity

The actual current-carrying capacity of a transmission line is limited by the ampacity of its hottest span. The location of the hot spot is constantly changing due to the variations in weather parameters along the circuit [30]. To identify the ampacity of each of the 200 spans, weather conditions with high spatial and temporal resolutions were used. Weather data for the entire year of 2008, with a time resolution of 10 minutes and spatial resolution of 1.2 km was derived from the weather research and forecasting (WRF) numerical weather prediction (NWP) model. Based on the derived meteorological values, the ampacity of each line span was calculated and the minimum ampacity for each time range was determined. The actual line capacity of the line varied from 656 A to 4643 A. Figure 3.2 demonstrates the line ampacity determined for July 2008.

Analysis of Results

The values of seasonal ratings calculated in the case study are presented in Table 3.2. Compared to the nominal static rating STRnom (900 A) usually accepted for the ACSR Drake conductor [42], the estimated seasonal ratings are significantly higher. For example, the minimum seasonal rating STRd for July (1192 A) is about 25 % higher than the deterministic rating. The maximum seasonal rating STRf for February (1517 A) is 40 % higher. Evidently, the established

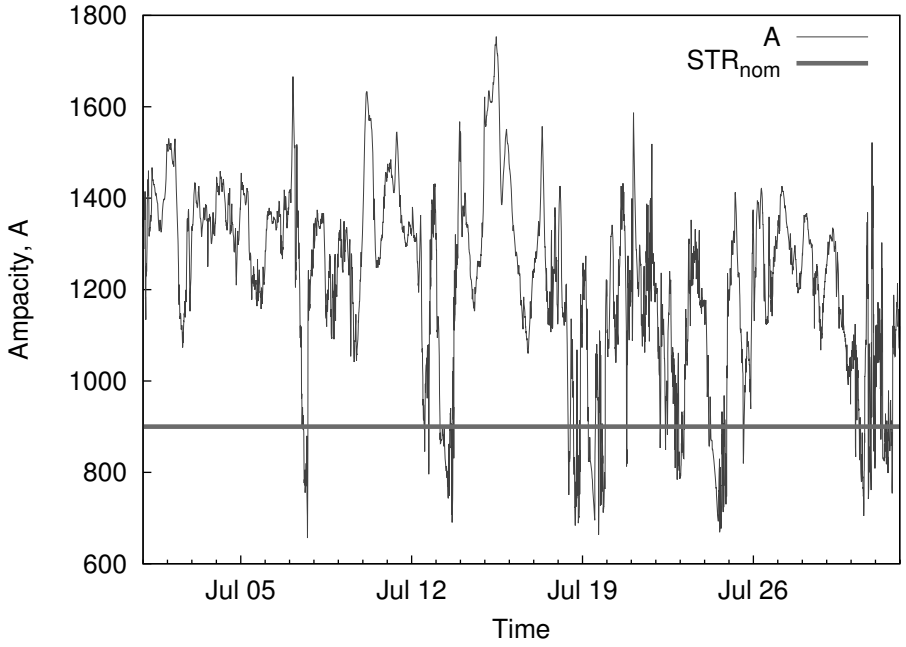

Figure 3.2: The estimated line ampacity for transmission line TL201 for July, 2008.

STR Label	time interval	STR, [A]	STR Label	time interval	STR day, [A]	STR night, [A]
STRa	year	1267				
STRb	summer	1236				
	winter	1410				
STRc	summer	1210	STRe	summer	1187	1237
	autumn	1311		autumn	1307	1317
	winter	1468		winter	1460	1477
	spring	1346		spring	1329	1365
STRd	January	1481	STRf	January	1480	1483
	February	1489		February	1460	1517
	March	1462		March	1461	1465
	April	1355		April	1333	1381
	May	1308		May	1294	1326
	June	1240		June	1222	1259
	July	1192		July	1164	1224
	August	1225		August	1199	1256
	September	1251		September	1248	1257
	October	1362		October	1359	1366
	November	1380		November	1379	1381
	December	1446		December	1447	1444

Table 3.2: Summary of calculated Seasonal Static Thermal Ratings.

seasonal ratings increase the transmission capacity of the line; however, they also increase the risk of thermal overload as shown in Figure 3.3. For a period of two weeks in June 2008, the deterministic rating remains below the actual line ampacity, while seasonal ratings are quite often higher than the line ampacity. This means that if the line were operated according to the seasonal ratings, the temperature of the conductor would rise above the thermal limit, accelerating aging of the conductor and the risk of possible network outage.

To more accurately estimate the impact of a seasonal rating on conductor thermal stress, the line temperature was calculated for all rating strategies (Table 3.1), assuming that the actual line current was equal to seasonal ratings. The calculations were performed for the entire year of 2008 based on the ambient weather parameters derived from the WRF model.

Figure 3.4 shows the frequency of conductor temperatures in the test line. It was assumed that the actual electric current is equal to the values of the seasonal ratings during the periods of time that the ratings represent. This case scenario makes it possible to quantify the risk of thermal overload for different rating strategies.

The results demonstrate that the conductor temperature exceeds the critical thermal limit of 95 °C about 20 % of the simulation time for most seasonal ratings. The same estimation for deterministic nominal static ratings is about 0.3 %, which confirms its large safety margins.

Summary

The main results of the case study are presented in Table 3.3. The values of average ampacity (AA) show that the transmission line, operated with the deterministic STR, is significantly underutilized; around 40 % of the potential line capacity idles. In contrast, seasonal STRs allow an increase in line throughput up to 96 % of the estimated ampacity average. With more alterations to seasonal rating (e.g., STRf – 24 alterations), the line utilization increases. However, the

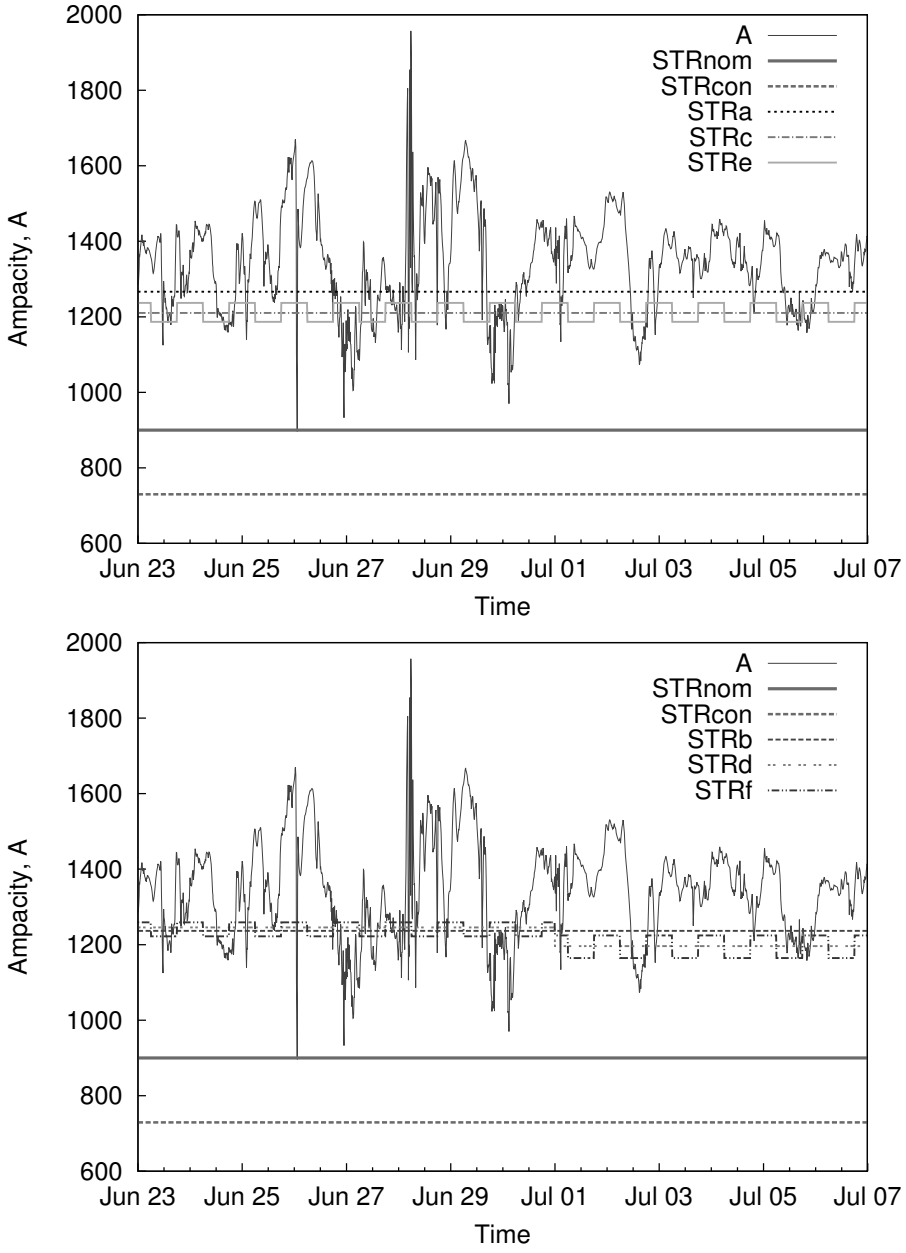

Figure 3.3: Seasonal Static Ratings STRa-f, nominal STR, and concervative STR for a period of 2 weeks.

capacity gain is not substantially different for the various seasonal rating strategies. For instance, the line throughput with STRf (24 ratings – 12 months and day/night shifts) is just 5 % higher than STRa (one thermal rating for a whole year).

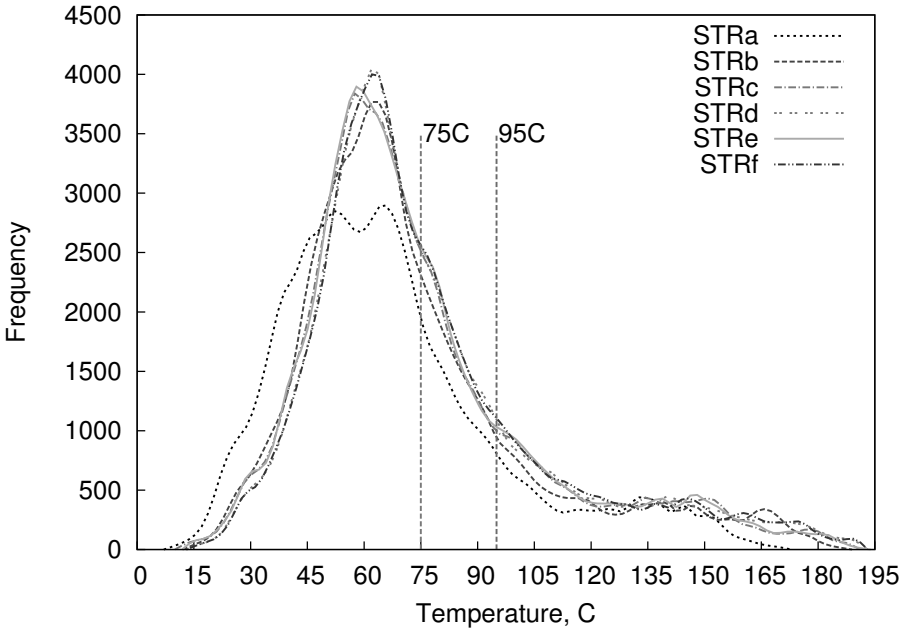

Figure 3.4: Frequency diagram of the conductor temperatures of the line operated with seasonal ratings STRa-f.

STR Label	Average ampacity (AA), [A]	Line utilization, % of AA	% of time $Tc \geq 95\,^{\circ}\mathrm{C}$
A	1408		
STRcon	729	52.8	0.0
STRnom	900	63.9	0.3
STRa	1267	90.2	14.7
STRb	1323	94.0	16.8
STRc	1334	94.7	19.9
STRd	1349	95.8	19.5
STRe	1335	94.8	19.5
STRf	1350	95.9	19.6

Table 3.3: Avarage ampacity and line utilization for deterministic STRs and seasonal STRs.

3.2.2 STR based on a Typical Meteorological Year

The probabilistic STR approach based on a typical meteorological year ($\mathrm{STR_{TMY}}$) was first introduced in 2000 [43]. The $\mathrm{STR_{TMY}}$ approach has been adopted as an alternative to deterministic STR by a number of utilities. It was shown in [43], [44], and [40] that an $\mathrm{STR_{TMY}}$ is usually higher than the nominal rating, which

makes it an attractive solution for thermal rating of transmission lines.

The source of weather information for the $\mathrm{STR_{TMY}}$ is a typical meteorological year dataset. A TMY is designed to represent weather phenomena for a specific location based on annual and long-term averages [45] For thermal rating calculation, a TMY is a source of typical weather conditions (wind speed, ambient temperature, solar radiation, etc.) in the area of the transmission line. A TMY dataset is comprised of the weather parameters for a period of one year with a time resolution of one hour. Such weather parameters are prepared through statistical analyses of real weather observations made during a long period of time (usually several decades).

The method of calculating the $\mathrm{STR_{TMY}}$ is similar to the method applied for the seasonal STR. It also is based on statistical analyses of the cumulative distribution functions (CDFs). The main difference is that for seasonal STR, CDFs are built from weather parameters, and for $\mathrm{STR_{TMY}}$, CDFs are created from ampacity values. The ampacity is calculated for all times of TMY weather data using IEEE-738 algorithms [35], then, the calculated ampacity is arranged in the form of a CDF. The final STR value is a value of a CDF percentile corresponding to a specified risk tolerance level (e.g., 5 %).

Although the $\mathrm{STR_{TMY}}$ approach seems to be an appealing alternative to the deterministic STR, a couple of critical issues must be analyzed before applying an $\mathrm{STR_{TMY}}$ to a system operation: (i) what is the actual risk of thermal overload for the $\mathrm{STR_{TMY}}$? and (ii) does the percentile, selected as a risk tolerance level, correspond to the actual risk of violating the thermal limit? These questions were not thoroughly investigated in previous research on the $\mathrm{STR_{TMY}}$ method [43],[40]. Other aspects of the $\mathrm{STR_{TMY}}$ approach must also be evaluated. How many locations with the TMY data are required to accurately calculate the thermal rating of a specific transmission line? How well does a TMY represent weather patterns of a surrounding region, and not just a single location? These and other questions are

considered in the following case study where the $\mathrm{STR}_{\mathrm{TMY}}$ approach is evaluated.

3.2.2.1 Case study

Assessment of a TMY-based static thermal rating was performed for power transmission line 5L081 (500 kV), located in the southern part of British Columbia, Canada, and operated by the electric utility BC Hydro. Figure 3.5 presents the test power line, three TMY weather stations (blue balloons), and two Weather Meteorological Organization (WMO) weather stations (white balloons).

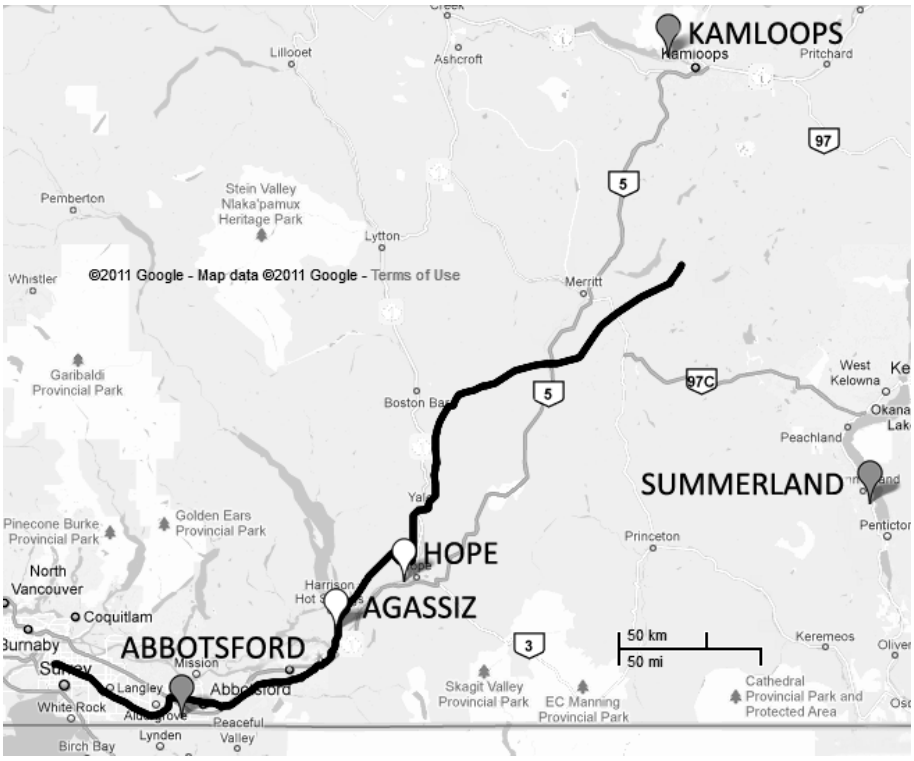

Figure 3.5: Study area in British Columbia for the STR-TMY case study.

In the current study, five advanced probabilistic thermal ratings (based on weather data from TMY datasets and historical weather observation archives) were calculated using the IEEE-738 algorithm. Calculation details and analysis of the results are presented below.

Description of the available sources of weather data

The typical year dataset used in the study is called Canadian Weather Year for Energy Calculation (CWEEC) [46]. The areas included in the dataset are represented by the darker balloons on the map in Figure 3.5. Each typical year is originally created by statistically processing 30 years of historical weather observations from the Canadian Weather Energy and Engineering Datasets (CWEEDS). The processed data are combined into 12 typical meteorological months which compose a typical year.

The two light balloons in Figure 3.5 show WMO weather stations located in close proximity to the sample line. The hourly observations from these stations represent the actual weather conditions along the circuit at the corresponding locations. Historical weather data from the meteorological stations were used to calculate the actual line ampacity for a period of 6 years (2005 – 2011). A summary of available data sources is shown in Table 3.4.

Station name	Data source	Time period of observations	0-wind speed observations
AGASSIZ	WMO station	6 years (20052011)	5678(11.2 %)
HOPE	WMO station	6 years (20052011)	3361(6.5 %)
ABBOTSFORD	CWEEC	1 typical year	1896 (21.6 %)
KAMLOOPS	CWEEC	1 typical year	1840 (21.0 %)
SUMMERLAND	CWEEC	1 typical year	1591 (18.2 %)

Table 3.4: Available weather datasets for the STR-TMY case study.

Estimation of Probabilistic Static Thermal Rating

The ampacity was calculated separately for five weather stations using corresponding weather datasets and location information. The latitude and elevation determined for each weather station were applied in the IEEE-738 algorithm to estimate an accurate thermal rating. Ampacities were obtained, sorted, and CDFs were built. Figure 3.6 shows the CDFs for the five weather stations. Figure 3.7 presents the same CDFs for the first 10 percentiles of the ampacity series.

The value of the final STR is derived based on a specified risk tolerance (the

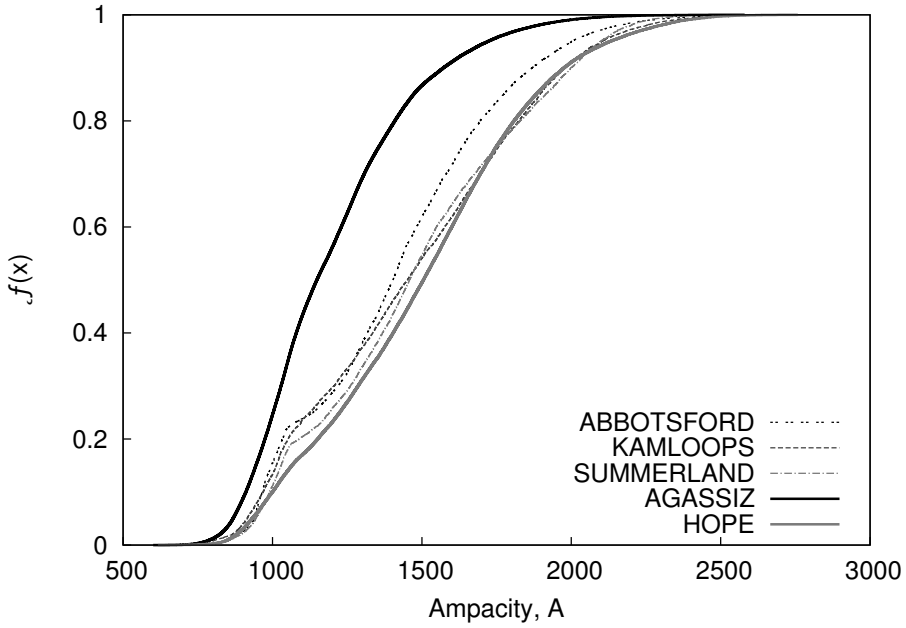

Figure 3.6: Cumulative distribution functions of an ampacity series derived from a CWEEC dataset.

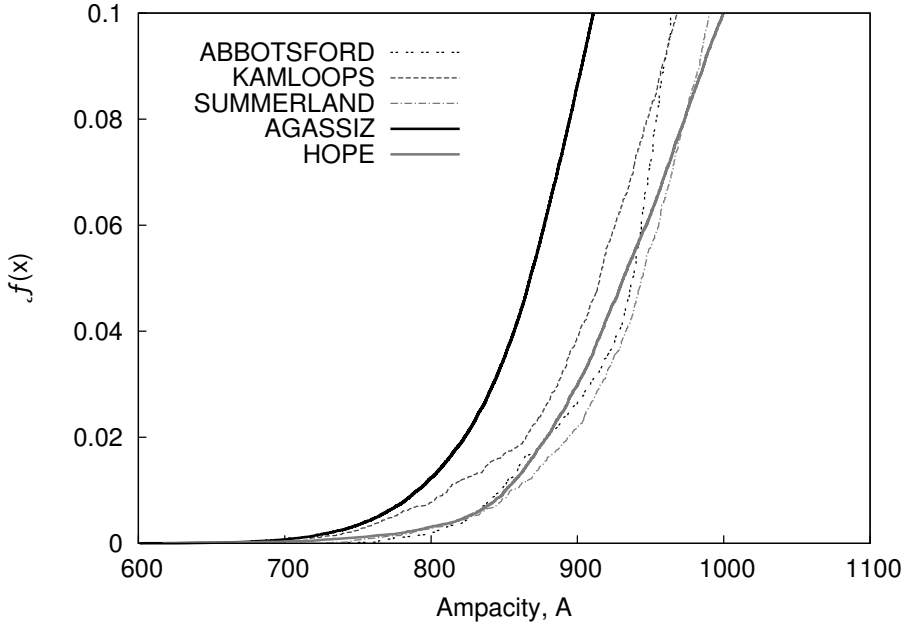

Figure 3.7: Cumulative distribution functions of an ampacity series derived from a CWEEC dataset (first 10 %).

risk that an electric utility is willing to acceptusually around $0 - 10\,\%$). The risk level corresponds to the percentile of the CDF, and the percentile value, in turn,

represents the value of the static rating. The STR_{TMY} approach requires that the calculated ampacities be consolidated into a single dataset [43]. The CDF built based on the ampacities of three TMY weather stations is presented in Figure 3.8.

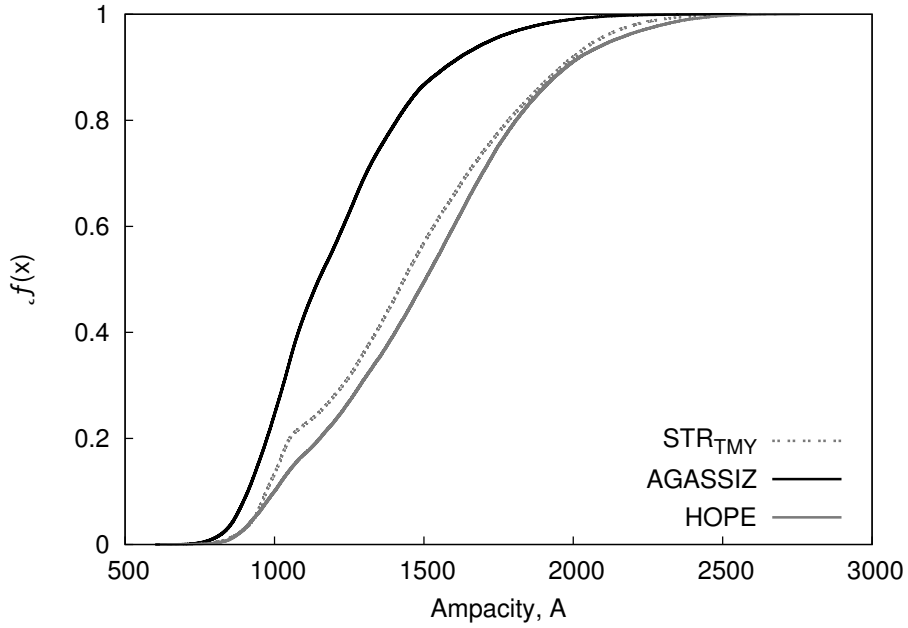

Figure 3.8: Cumulative distribution functions of actual ampacity series at two line spans and an ampacity series derived from a CWEEC dataset for STR_{TMY}.

Analysis of results

Table 3.5 contains probabilistic STRs estimated for different risk levels. The first two columns show STRs calculated based on 6 years of historical weather observations. The next three columns of Table 3.5 present STR_{TMY} values calculated using a Typical Meteorological Year dataset separately for different weather stations. The last column is a final probabilistic STR_{TMY}.

Similar to the study of seasonal STRs, new probabilistic STR_{TMY} values were compared to deterministic STRs: STRcon (729 A) and STRnom (900 A). It can be seen from Table 3.5 that STR_{TMY} values that correspond to risk levels higher than 0 % are higher than the conservative STRcon (729 A). If the risk tolerance level is higher than 5 %, then the STR_{TMY} is even higher than STRnom (900 A). The capacity of the line operated under the new STR_{TMY} is increased. Studies [43],

Percentiles	STRs based on the location					
	AGASSIZ	HOPE	ABBOTSFORD	KAMLOOPS	SUMMERLAND	STR_{TMY}
0 %	601	617	739	650	728	650
1 %	791	851	849	811	855	840
2 %	823	879	880	865	894	877
5 %	868	931	938	915	944	933
10 %	911	1000	964	968	991	973

Table 3.5: Results of probabilistic static thermal ratings calculations.

[44], and [40] showed more significant increases in STR_{TMY} values. The actual gain in the rating depends on a particular geographical area and local weather patterns presented in the form of a typical meteorological year. The results also show that probabilistic STRs derived from actual line ampacity (the first two columns of Table 3.5) in most cases are lower than the STR_{TMY} values. The risks of STR_{TMY} are underestimated, which, in the operation of a real system, can cause violation of the thermal limit.

Analyses of the CDFs (Figure 3.7 and Figure 3.8) and the final probabilistic STRs (Table 3.5) show that the ampacities at different locations are different. The probabilistic STR depends on which weather stations were used in the calculations. An STR_{TMY} based on weather data from all available weather stations will differ from STR_{TMY} estimated for separate stations. A result that is dependent on a particular dataset contains a great deal of uncertainty. It is not possible to conclude how many TMY datasets are necessary and which locations must be considered to remove this dependency. Even probabilistic STRs calculated using historical weather data from two relatively close weather stations are quite different. This suggests that local weather patterns may be quite different and that describing them with average parameters of a typical meteorological year can lead to misleading and unreliable ratings.

3.2.3 Assessment of static thermal rating

The results of the case studies presented in the previous subsections demonstrate that probabilistic thermal ratings are usually higher than deterministic ratings. With a seasonal rating or a rating based on TMY weather data, the capacity of a transmission line increases allowing an electric utility to transfer more energy than with a conventional rating. Another advantage of probabilistic STRs is that they are provided with risk levels of thermal overload. An electrical utility can select a rating based on its statistically determined risk levels rather than on assumptions of unfavourable weather conditions, the basis of a deterministic static rating. However, it was shown that such risks might be underestimated, leading to violation of thermal limits and reducing the reliability of the entire transmission system.

The major drawback of the probabilistic approach is that there is no guarantee that the historical weather data (observations from weather stations or typical meteorological year data) used for the calculations can represent actual weather conditions along the transmission circuits. In other words, there is no means to justify the accuracy of the risk levels obtained from the available weather data. It is likely that weather patterns (due to the specific landscape, vegetation coverage, etc.) along the transmission lines differ greatly from weather conditions observed at the weather stations. Although probabilistic thermal rating is a better alternative to deterministic thermal rating from the point of view of line utilization, it exposes the transmission line to a risk of violating the thermal limit.

3.3 Dynamic Thermal Rating (DTR)

If the actual weather conditions along a power transmission line are known, it is possible to estimate a thermal rating close to its actual limits. Dynamic thermal rating (DTR) provides real-time thermal rating based on current weather

parameters. The DTR is the maximum allowable electric current in a power line assuming that the conductor is at its maximum allowable temperature. As ambient weather conditions vary with time, the DTR changes as well. Ampacities differ along the circuit due to variation in local weather patterns. The ability of the DTR approach to capture the actual maximum current of the line provides significant advantages over STR approaches. Most of the time, the true line ampacity is higher than the conservative deterministic STR [47], [3]. A DTR allows an electric utility to deliver more power with high reliability and safety. The reliability of the DTR is achieved because all weather scenarios (including the worst-still wind and high ambient temperature) are picked up during the calculations. In comparison, statically rated power lines can violate thermal limits during times when ambient conditions are more adverse than those used for the STR estimation. STRs are based on fixed, conservative but not worst, weather assumptions. DTRs are based on actual weather conditions and thus allow safe line operation.

Over the last a few decades, DTR techniques have been proposed and DTR systems have been created and tried by many utilities in different countries. Although several DTR approaches have been implemented in commercial products, there is a lack of consensus concerning which technique performs the best [8]. DTR approaches can be divided into the following five categories: (1) weather based [24], (2) tension based [15], (3) sag based [14], (4) conductor temperature based [16], and (5) replica conductor based [13]. Section 3.3.1 reviews some of these methods.

3.3.1 Existing DTR systems

3.3.1.1 Remote weather stations (weather based DTR system)

Remote weather stations can be used to collect weather parameters along the circuit in real-time. For the purpose of DTR, weather stations are usually installed on transmission towers to measure the weather conditions the line is

exposed to. Typically, a weather station can measure and record a variety of weather parameters including those critical for a DTR calculation: peak wind speed and direction, average wind speed and direction, solar radiation, and ambient temperature. Input parameters for algorithms of the DTR calculation are observed weather parameters and characteristics of the conductor. In North America, IEEE Standard 738 [35] is used to rate lines with weather data. CIGRE standards [38] are used in Europe.

Remote weather stations require a constant power supply for saving observations on a storage device. Typically, a solar panel and a battery are installed together with the weather station on a tower. Reliability and confidence of the DTR system depends on the reliability of the solar panel and the sufficiency of the battery during times of low daylight.

3.3.1.2 Arteche SMT (conductor temperature based DTR system)

The Arteche SMT DTR system is based on a temperature measurement sensor developed by the Spain-based company Arteche. The SMT device is installed directly onto the transmission line, so that it embraces the conductor. Using the electromagnetic field of the line, the device can not only measure the current passing through but also the power itself. The thermocouple of the SMT measures the temperature of the conductor. A minimum line current of 60 A is required to record measurements and communicate with the datalogger (storage place). Arteche SMT can store up to 1000 data entries (approximately one week) on a local flash memory before they must be sent to a remote storage location.

Information about conductor temperature is not enough to calculate the DTR. Arteche SMT requires ambient weather conditions to estimate a thermal rating. The conductor temperature and electric current measured by the SMT are combined with the weather data observed at the weather station and the dynamic rating is calculated using a CIGRE algorithm.

3.3.1.3 EDM Sagometer (sag based DTR system)

As an increase in the temperature of the conductor increases the sag of the line, it is possible to use this information to derive dynamic rating values. The sagometer measures the sag of the line, calculates the conductor-to-ground clearance (at the lowest point of the line), and combines this information with weather data to estimate the conductor rating. The sagometer consists of a camera mounted on the transmission tower and a target mounted on the line. The camera lens points to the target and detects its movement when the sag of the conductor increases or decreases. The camera is able to see the target in fog and at night as well as in daylight. A sufficient power supply must be provided to assure reliable data collection.

3.3.1.4 ThermalRate (replica conductor based DTR system)

The ThermalRate DTR system uses a conductor replica to identify the maximum safe electric current by evaluating the impact of ambient weather conditions on the replica. The device contains one "cold rod"a conductor replica that remains unheated, and one "hot rod" – a conductor replica that is constantly heated. By calculating the cooling effect of the "effective" wind, wind turbulence, precipitation, and other factors on the hot rod, the DTR is calculated. Knowing the effective wind speed together with the characteristics of the actual conductor (not the replica), the ThermalRate uses the IEEE 738 Standard to calculate a rating. The ThermalRate has all the necessary weather sensors, so it does not require weather data from other systems (e.g. a remote weather station). The ThermalRate requires a constant power source (17 W, 24/7 for 365 days) to heat the hot rod. For some locations a solar system must be installed.

3.3.1.5 Summary

The observed DTR systems, in general, provide ratings with accuracy sufficient for reliable system operation. However, the estimated rating is based on the weather patterns at a single location. Remote weather stations observe local weather parameters; the ThermalRate system calculates DTR based on the effective wind at the location where the device is installed, the EDM Sagometer measures the sag of a single span. In other words, available DTR systems provide span DTRs which may or may not be equal to the ampacity of the line. As weather conditions continually change along the line, the worst conditions may escape detection. To increase the accuracy of the estimated rating, DTR systems must be installed across the entire line, but the cost and complexity of DTR installation at each line span is too high to be realistic.

Advanced DTR systems are based on numerically simulated weather data. A weather research and forecasting (WRF) numerical weather prediction (NWP) model is used to provide weather parameters of high spatial and time resolutions for each span of the line. The benefit of the system is the ability to provide a DTR based on the worst weather conditions detected along the entire line. In addition, the forecasting of weather conditions allows more accurate planning and scheduling of the load patterns based on the estimated current-carrying capacity of the line.

3.3.2 Advanced DTR system based on Numerical Weather Prediction (NWP)

An advanced dynamic thermal rating system that relies on the high resolution mesoscale NWP model was proposed in [1]. This DTR approach allows accurate estimation of real-time line ampacity as well as reliable ampacity forecasts. The structure of the advanced dynamic thermal rating (ADTR) system is

presented in Figure 3.9. The main system components are (1) the NWP model including analyses forecasts and initialization data, (2) modules responsible for data preprocessing and DTR algorithms, and (3) a database.

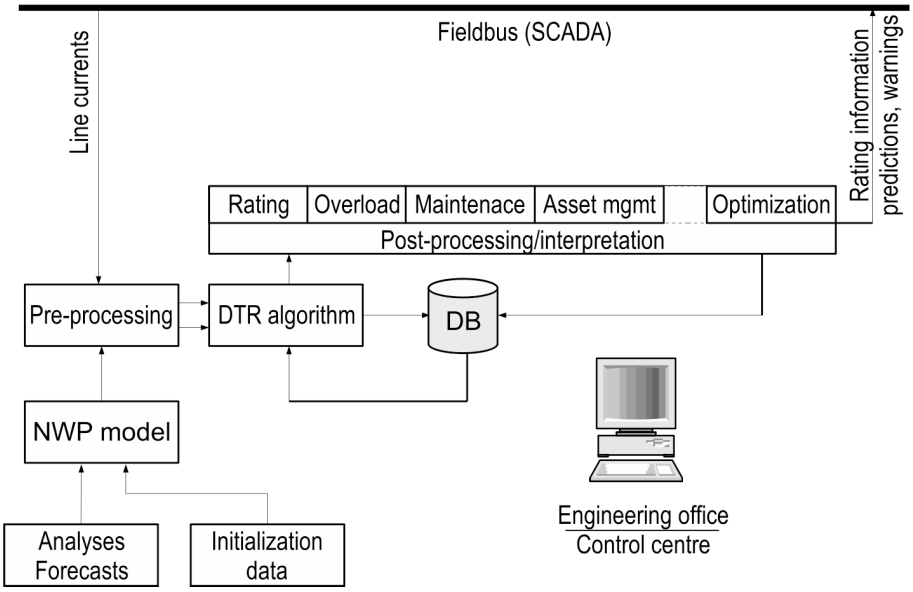

Figure 3.9: Structure of an advanced DTR system (image retrieved from [1]).

As the advanced DTR system relies on NWP weather data, the potential inaccuracy of weather forecasts can lead to inaccurate DTR calculation. To reduce errors in the NWP model and increase the reliability of the system, model output statistics (MOS) are applied. The next chapter evaluates MOS and presents a case study that applies MOS.

Chapter 4

Application of Model Output Statistics (MOS) to improve the NWP-based DTR System

The advanced DTR approach investigated in the current research is based on a numerical weather prediction (NWP) model (hereafter, DTR-NWP or NWP-based DTR). The accuracy and reliability of the DTR-NWP system depends on the accuracy of weather simulations. If the weather parameters of the model clearly indicate the actual weather conditions at each point of a specified area, then the calculated dynamic thermal rating will be very close to the actual line ampacity. Uncertainties in the numerical weather simulations of any NWP model are inevitable [48]. They introduce errors in the DTR calculations and these errors diminish the value of the DTR-NWP system. To reduce errors in rating estimations, the errors in the NWP model must be reduced. That can be achieved by applying a model output statistics (MOS) technique. MOS reduces errors in the model and significantly improves the accuracy of numerical weather simulations.

4.1 Principles of MOS

Numerical weather prediction models have been improved significantly since their first operational applications in the 1960s, but the accuracy of the predictions still requires refinement [48]. Model output statistics are applied to reduce the bias and inaccuracy of the numerical model and improve numerical weather forecasting.

4.1.1 NWP limitations

Existing numerical weather prediction models provide an approximation of atmospheric behaviour. Some physical processes happen on a scale too small to be detected by the numerical models. In other cases, physical processes are too complicated to be described precisely by the mathematical equations. But even if a perfect model of the atmosphere could be built, it would be impossible to avoid uncertainties (errors) in predictions. The reason for this is a so-called dynamical chaos. The main idea of chaos theory is that slight changes in initial parameters of a complex nonlinear dynamic system will change the behaviour of this system drastically over time. Since it is not possible to determine absolutely perfect initial conditions for the numerical model (observations of the atmosphere always contain some errors), it is not be possible to predict the state of the atmosphere without uncertainty. Despite this fact, numerical weather prediction is a widely used, promising technique that has improved significantly with research and practice [48].

4.1.2 MOS overview

Uncertainties (errors) in the weather forecasting of the NWP model can be reduced with MOS, a statistical postprocessing technique first introduced in the 1970s [49]. MOS is currently used to improve the results of global NWP models and provide guidance to weather forecasting bureaus [50].

The main steps of the MOS procedure are: (1) The relationship between a weather parameter predicted by a model and the actual weather condition that corresponds to the prediction is derived. Such a relationship is called a regression model and it is expressed in the form of a linear equation. (2) For each weather parameter that needs to be improved (air temperature, wind speed, humidity, etc.), and for each required forecasting horizon (6 hours, 12 hours, 18 hours, etc.), a regression equation is built. (3) After the statistical equations have been derived, they can be applied to improve the newly simulated weather parameters from the numerical model.

4.1.3 Predictors and predictands

A predictand is the prediction of a weather parameter. A predictor is a variable that is used to derive the predictand. Usually, more than one predictor is used to establish the statistical relationship between the predictand and the relevant variables from the NWP model. For example, if the task is to build a regression model (a statistical relationship) for an ambient temperature, then the predictand will be the air temperature that must be identified and the predictors will be the variables provided by the NWP model.

The available data used to build a regression model – weather observations and, corresponding to them, numerically simulated weather parameters – are called the developmental sample, dependent sample, or training sample. The bigger the developmental sample, the more statistically accurate the MOS model will be.

The selection of potential predictors is an important step in building a regression model. It is important to choose predictor variables that are physically meaningful to the predictand. Choosing too many predictors in a forecast equation can cause data overfitting [48], [49].

4.2 Linear regression

Model output statistics is essentially a multiple linear regression procedure performed on the output of an NWP model and historical weather observation data. MOS equations are linear functions that describe linear relationships among the variables: the weather parameter that must be improved and related variables simulated by the NWP model.

Multiple linear regression is a statistical procedure that determines a relationship between a stochastic variable Y and a set of random variables (X_1,X_2,X_3,,X_n). The variable Y is called the predictand, or dependant variable, as it depends on variables X_1,X_2,X_3,,X_n, which are called independent variables or predictors.

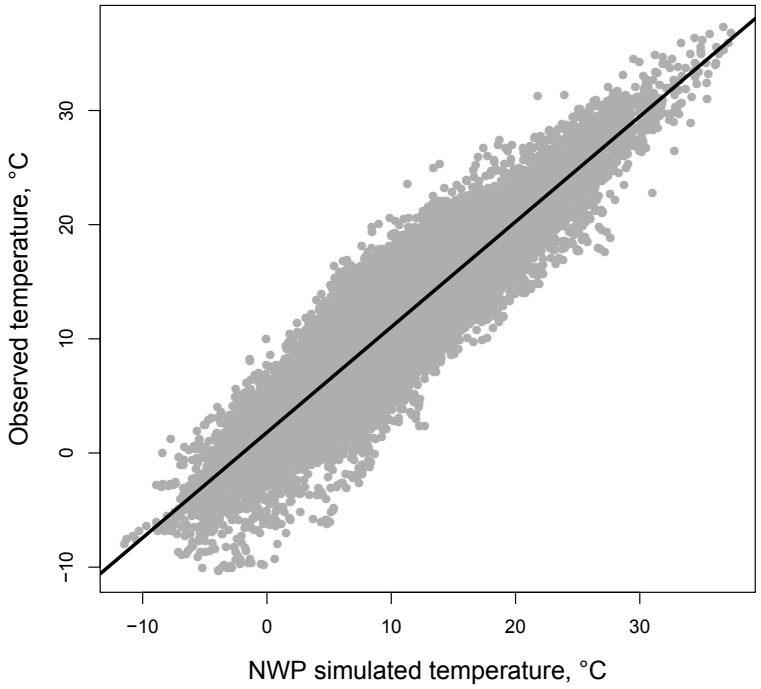

Figure 4.1: Scatterplot of numerically simulated and observed air temperature.

The scatterplot in Figure 4.1 demonstrates the relationship between the actual observations of air temperature and the temperature simulated by the NWP model. The plot was built using observations from the AGASSIZ weather station (British Columbia, Canada) and the output from the WRF model at the location

of the weather station. The time period is three years – 2007, 2008, and 2009. There is a strong linear relationship between observed temperature Y and predicted temperature X. If the predictions were absolutely correct we would see the straight line drawn with a 45 degree angle to the axes. Due to uncertainties in the numerical simulations, we see a cloud of points distributed along an imaginary line. The actual relationship between X and Y is described by a certain unknown function $y = f(x)$. The linear regression procedure creates a linear function $\tilde{y} = \tilde{f}(x)$, which is an approximation of the actual function $y(x)$. The regression function is derived in such a way that the sum of the squares of the estimation errors is minimal $\sum_{i=1}^{n}(y_i - \tilde{y}_i)^2 = minimum$. The regression function obtained for the current example is $y = 1.8018 + 0.9227x$ (*); it is represented by a line in Figure 4.1.

After the regression function is constructed, it can be applied to estimate the actual temperature based on data provided by the NWP model. For example, if the output of the NWP simulation is $x = 15\,^{\circ}\mathrm{C}$, the equation (*) returns 15.64, which is the actual air temperature y (after rounding it is $16\,^{\circ}\mathrm{C}$). The linear equation always returns the same output for the same input; thus, it is an objective weather forecasting technique. As shown in Figure 4.1, when NWP predicts the temperature $15\,^{\circ}\mathrm{C}$, the actual temperature value varies over a certain range.

4.3 Screening procedure

Due to the fact that the potential predictor variables almost always correlate to each other, it is not useful to include all of them in the final equation. Inclusion of mutually correlated predictors into MOS development causes poor estimates of the predictands [48]. If the model is overfit by too many predictors, the predictand may be estimated well in the dependent data sample, but the model will perform poorly based on the independent data [49]. The regression is screened to identify predictors that produce a good regression equation. Goodness of the equation

in this context is a maximum reduction of variance or, equivalently, a maximum reduction of the sum of squares of the estimation errors [49]. The most commonly used screening procedure is known as forward selection, or stepwise regression.

The initial state of the screening procedure is an uninformative prediction equation $\tilde{y} = b_0$. The only intercept term represents the sample mean of the predictand. In the first step of the forward selection, for each of M potential predictors a simple linear regression equation is built. All M regressions are examined to identify the one that is the best (strongest) among all candidates. The predictor whose linear regression appears to be the best is included in the developmental prediction equation $\tilde{y} = b_0 + b_1 x_1$. The variable x_1 correlates to the predictand the most strongly and thus explains a greater fraction of the predictand variance [49]. At this stage b_0 is an intercept and no longer an average of the value y.

In the next forward selection step, remaining $M - 1$ predictors participate in building linear regression equations for the predictand $\tilde{y}$, but all the trial regressions also contain the predictor x_1 identified in the previous step. Similar to the first selection, the strongest linear regression is selected, and the predictor x_2 of this equation is included in the developmental model – $\tilde{y} = b_0 + b_1 x_1 + b_2 x_2$.

Subsequent steps in the screening procedure follow the algorithm described above. The predictors that are not yet in the regression model are examined for their contribution to the final regression equation, so that the regression demonstrates the strongest linear relationship with the predictand. Without a stopping criterion, a screening procedure continues until all potential predictors M are included in the final MOS model. The stopping rule is usually a cutoff value of an additional reduction of variance conveyed by a newly selected predictor.

4.4 Methodology of MOS application in the DTR-NWP system

The DTR-NWP system incorporates weather predictions of the WRF model for calculating the thermal rating of a transmission line. Accuracy and applicability of the system essentially depend on how well numerical simulations can represent true weather conditions. Criteria for estimation accuracy of the NWP model and methodology to improve the DTR-NWP system through MOS application are described below.

4.4.1 Accuracy of the NWP model

Accuracy of the NWP model is considered in a different way for DTR than for regular weather forecasts. Predictions are counted as errors only if they increase the risk of violating the thermal limit. For example, underprediction of air temperature (the actual temperature is higher than the forecasted one) or overprediction of wind velocity (the actual wind speed is lower than the predicted one) produces an increase in the lines thermal rating beyond its actual ampacity. Such a result is a critical error because it leads to conductor overheating. Alternatively, when ambient temperature is predicted to be higher than it actually is, or wind speed is underestimated by the model, the final thermal rating will be below the actual line ampacity. There will be no risk of line overheating, but the potential current-carrying capacity will not be fully utilized. Underestimation of the thermal rating, while undesirable, is not a critical error, and weather simulations included in such results are acceptable in the NWP system.

Accuracy of wind direction simulations must also be considered differently in the DTR-NWP system compared to regular weather forecasts. The angle of incidence of wind to a power line has a critical effect on DTR calculations. However, the same angle of incidence can be achieved with four different wind directions (or

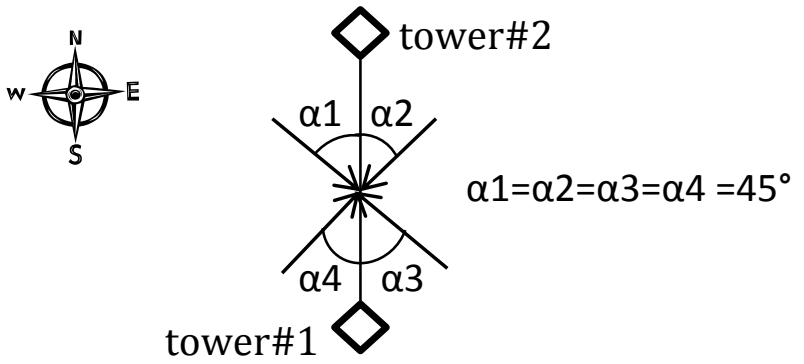

Figure 4.2: Wind direction with respect to a power transmission line span.

two wind directions in a case of strictly parallel or perpendicular wind), as shown in Figure 4.2.

A single line span and four possible wind directions are depicted in Figure 4.2. Wind blowing from four different directions equally cools the conductor as long as the angle of incidence to the line remains the same. In Figure 4.2, $\alpha_1 = \alpha_2 = \alpha_3 = \alpha_4 = 45\,^{\circ}\mathrm{C}$, which means that all of the predicted wind directions (45 °C, 135 °C, 225 °C, and 315 °C) are correct results. In contrast, for a regular weather forecast, only one value would be counted as the correct response.

4.4.2 Methodology of MOS application

Weather simulations in the DTR-NWP system are predicted by the numerical model. The three most important weather parameters required for thermal rating calculations are ambient temperature, wind speed, and wind direction. Other weather variables that would be beneficial to the rating estimation but are not strictly necessary are amount of solar radiation, precipitation rate, relative humidity, and air pressure. These parameters can increase the accuracy of the thermal rating calculation as they include the impact on a conductor of solar heating and precipitation cooling. Without these four extra parameters, the estimated rating is always equal to or less than the actual line ampacity.

The WRF model, the main component of the DTR system, produces all the variables required for the rating calculation. Due to unavoidable uncertainties in the numerical weather simulations, the output from the WRF model contains errors. Such errors can be partially reduced by postprocessing with MOS. Application of MOS to improve the accuracy of temperature and wind impacts on the DTR was investigated.

The MOS model is built using historical weather observations (predictands) and WRF weather simulations (predictors). The obtained MOS equations are tested on an independent dataset. If the MOS regressions demonstrate an acceptable reduction of error, they are applied to weather forecasts newly simulated by the WRF model. The accuracy of the weather simulations must be constantly monitored to ensure numerical simulations represent true weather conditions.

4.5 Case study

A case study was performed to evaluate the enhancement of the NWP-based DTR system by MOS. Particularly, the goals of the study were to estimate improvements in accuracy of the numerical weather simulations after applying MOS and to analyze how these improvements affect dynamic thermal rating calculations. The case study involves seven steps .

(1) Identify the area of the study and perform numerical weather simulations for this region.

(2) Evaluate available data sources of the historical weather observations in the area of interest and prepare datasets with the required weather parameters (ambient temperature, wind velocity, wind direction). Such data sources are typically meteorological weather stations located in close proximity to the transmission circuits.

(3) Postprocess historical weather observations. Zero wind direction and zero wind speed must be modified to avoid the significant bias they introduce in the rating calculation.

(4) Postprocess WRF simulations so that the precision of the WRF variables are the same as the precision of the historical observations. This step is required in order to perform adequate assessment of simulation accuracy and build MOS equations accounting for the limitations of the accuracy of actual weather observations.

(5) Calculate a thermal rating using WRF data and real weather measurements. The results will demonstrate the accuracy of the DTR-NWP approach.

(6) Apply MOS to reduce errors in weather simulations and compare the improved results with the original WRF output.

(7) Calculate a thermal rating based on the enhanced NWP weather data and evaluate how the improvements in the weather parameters affect the accuracy of the thermal rating.

4.5.1 Test site

Three requirements for the potential test site were: (1) presence of high-voltage power transmission lines, (2) diverse geography, and (3) availability of at least two meteorological weather stations that collect weather data hourly and keep historical observations for at least three consecutive years.

The first requirement assures practical value of the study. The second criterion allows evaluation of WRF model accuracy in a challenging environment. Numerical weather simulations for mountainous regions are usually less accurate than simulations for flat areas; the more complex physical processes in the atmo-

sphere of a mountainous region (compared to a flat region) engenders more complex numerical solutions of the nonlinear equations generated in the analyses. The last requirement, the availability of historical weather data, is important for building MOS equations and examining the accuracy of numerical simulations. The longer the period of actual weather observations, the more statistically representative and reliable the final results will be.

Based on the requirements specified above, a test site was identified. The southern part of British Columbia, Canada, was selected for the study (Figure 4.3).The area contains a diverse landscape with land elevations from a few meters to several kilometers. The red line on the map in Figure 4.3 shows a 500 kV power transmission line (5L081) operated by the electric utility BC Hydro. The two baloons represent World Meteorological Organization (WMO) weather stations in AGASSIZ and HOPE , with available historical hourly weather data for a period of 6 years (2005 – 2010).

4.5.2 WRF domain

The weather research and forecasting (WRF) NWP model, the main component of the advanced dynamic thermal rating system, was used for numerical weather simulations in the area of the transmission circuit. The WRF model was set up for the selected area in British Columbia. There are three nested domains, each of different spatial resolution (Figure 4.4): an outer domain, 10.2 km (blue square); a middle domain, 3.6 km (yellow square); and an inner domain, 1.2 km (red square). This type of WRF configuration (three nested domains) is commonly used and provides good performance in the model.

The inner domain (Figure 4.5) has the finest resolution among all three regions, so data from this domain were applied to build MOS equations and calculate a DTR for the sample power line. The first seven grid points from each side of the domain are boundaries; the weather simulations at those locations are not accu-

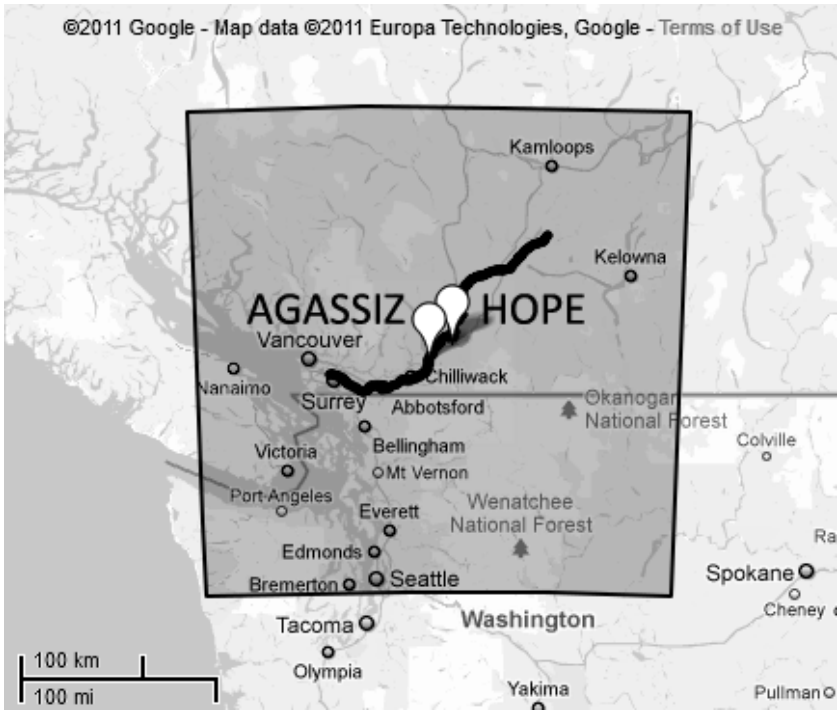

Figure 4.3: The case study area (British Columbia, Canada), including power transmission line 5L081 and WMO weather stations located in close proximity to the circuit.

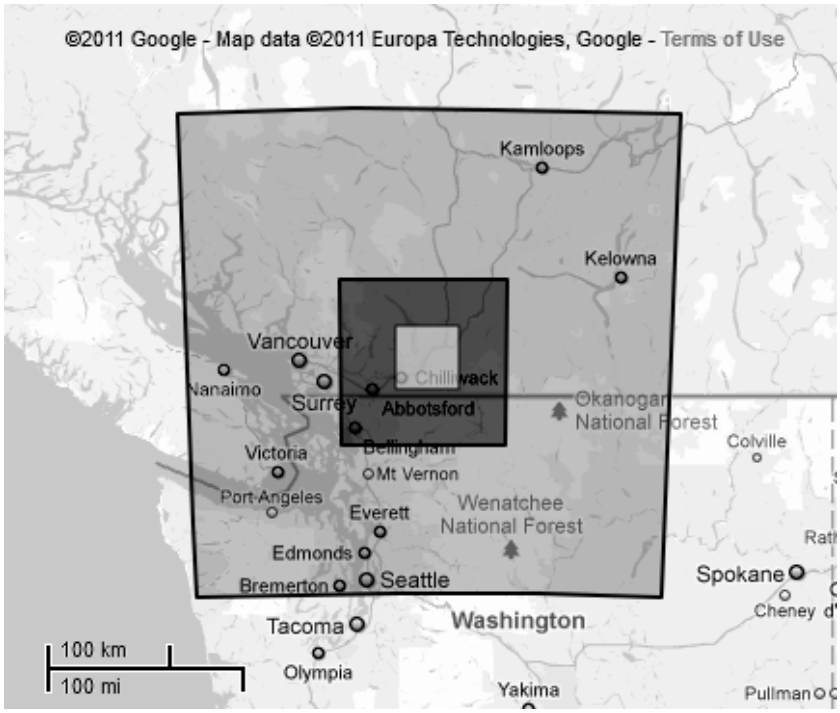

Figure 4.4: Three nested domains of the WRF setup.

rate due to the changes from coarse spatial resolution to fine resolution. Weather parameters from the boundary layers were not used in the calculations. The inner dark polygon in Figure 4.5 shows the actual area used.

The sample power line 5L081 crosses the domain; 155 towers of the line are covered by the reduced WRF domain (Figure 4.5). A dynamic thermal rating was calculated for each of 155 line spans, accounting for the line heading and elevation of tower locations.

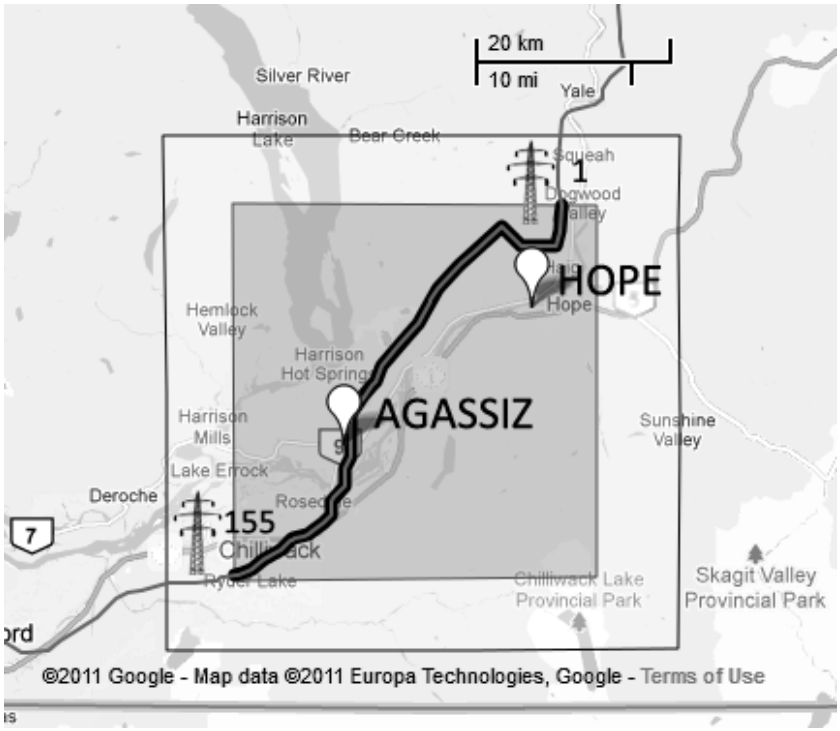

Figure 4.5: The inner domain of the WRF setup, including the 5L081 power transmission line and WMO weather stations.

Figure 4.6 depicts areas with meteorological weather stations. The grid point closest to the actual location of the meteorological station is showen as a balloon with a dot inside. Simulated weather data from those grid points were extracted for MOS calculations and assessment of accuracy of the WRF model.

Figure 4.6: Enlarged areas of the weather stations (AGASSIZ – left, HOPE – right) with marked grid points nearest to the weather stations.

4.5.3 Available historical weather data

Actual weather observations are required to build MOS equations. Two sources of historical weather data were originally considered for the study. The first data source was a Research Data Archive (RDA) maintained by the Computational and Information Systems Laboratory (CISL) at the National Center for Atmospheric Research (NCAR) [51]. It contains hourly observations from about 1000 stations in the U.S., Canada, Mexico, and most countries in Central America. The second source was Environment Canada (EC) National Climate Data and Information Archive [52], available online and covering all meteorological weather stations inside Canada.

It was assumed that the data provided by both sources must be identical for the same weather stations; however, a quick quality check of both datasets revealed that the RDA data are filtered and interpolated. Figure 4.7 clearly illustrates that the EC weather observations are more accurate and representative than those in the RDA dataset. Finally, the EC historical weather archive was selected for the case study.

Hourly weather measurements from the two WMO weather stations were downloaded and prepared for the case study. The original dataset contains 10

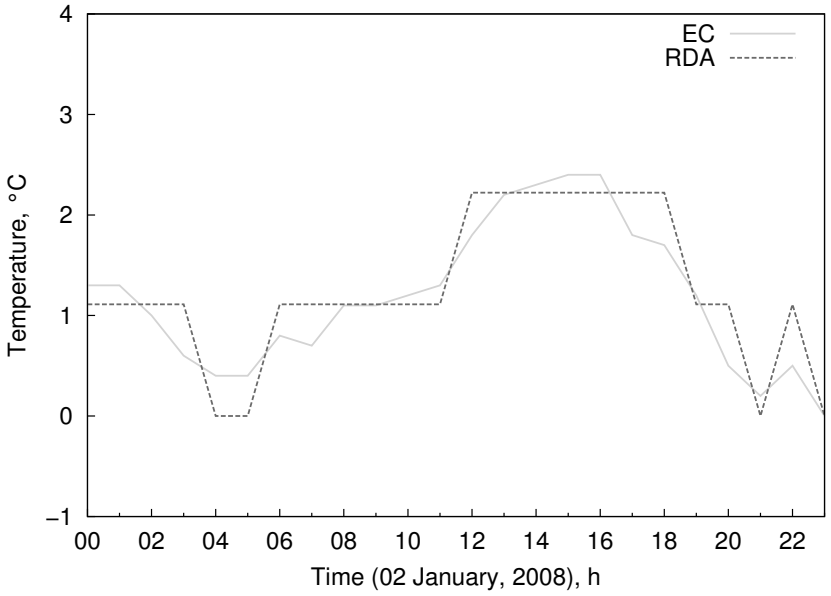

Figure 4.7: Comparison of EC and RDA historical weather observations.

weather parameters, three of which were used in the study: ambient temperature, wind speed, and wind direction. The main characteristics of the available historical weather data are presented in Table 4.1.

Weather station	Start year	End year	Hours of observations	Missing data for the period of observations	Zero-wind speed observations
AGASSIZ	2005	2010	50847	1737 (3.4 %)	5678(11.2 %)
HOPE	2005	2010	52015	569 (1.1 %)	3361(6.5 %)

Table 4.1: Main characteristics of available historical weather observations from two weather stations AGASSIZ and HOPE.

4.5.4 Post-processing of historical weather data and WRF simulations

The precision of WRF weather simulations is significantly higher than the precision of weather observations from the meteorological weather stations. For example, wind speed measured at the AGASSIZ and HOPE stations is presented as discrete values with the resolution of 0.56 m/s (2 km/h). The lowest wind speed

recorded at the AGASSIZ station is 0.56 m/s (2 km/h) and at the HOPE station 1.11 m/s (4 km/h). For accuracy estimation, NWP simulations were rounded to have the precision of EC data. Ambient temperature was rounded to one significant figure. Wind velocity is approximated to the discrete values of the historical weather data (0.56 m/s, 1.11 m/s, 1.67 m/s, 1.94 m/s, etc.). Wind direction was divided into 36 possible directions, from 10 to 360 degrees. Zero wind direction (similar to zero wind velocity) in the dataset of historical observations means that the wind was too low to be identified accurately with an anemometer. Such wind measurements were changed to 0.4 m/s and wind direction was interpolated between previous and next available wind directions. Low-wind wind speed provided by the WRF model was not changed to preserve its high precision.

Environment Canada weather data were filtered to remove data points where at least one of the weather parameters (ambient temperature, wind speed, or wind direction) was missing. Additional checking was performed to assure that all variables were in acceptable ranges (e.g. wind speed is higher than 0).

4.5.5 Application of MOS

MOS regression equations were built for the WRF model variables using actual weather observations from the two weather stations – HOPE and AGASSIZ – and WRF numerical weather simulations extracted from the model grid points closest to the weather stations (balloons with dots in Figure 4.6).

4.5.5.1 Predictands

As the MOS are applied to improve the accuracy of the DTR, only three predictands are considered in the current case study: ambient temperature, wind speed, and wind direction. These are the most important parameters affecting ampacity calculations. The amount of solar radiation predicted by the WRF is another essential variable that requires improvement. However, the dataset with

historical weather observations from two meteorological weather stations did not contain observations of solar radiation; therefore, it was not possible to build regression equations for solar radiation. A solar model instead of actual observations of solar radiation was used for ampacity calculations.

4.5.5.2 Predictors

The MOS procedure for building regression equations requires a selection of potential predictors. In the current case study the predictor pool contained 44 WRF variables:

- simulations of ambient temperature at 2 meters above the ground as well as at various pressure levels (925 mb, 950 mb, 850 mb, 700 mb, and 500 mb);
- relative humidity, dew temperature, and moisture content at 2 meters above the ground;
- surface and sea level air pressure;
- horizontal vector components (U, V) and a vertical vector component of wind (W) as well as derived values of wind velocity and wind direction at 10 meters above the ground (surface wind) and at various pressure levels (925 mb, 950 mb, 850 mb, 700 mb, and 500 mb).

The predictors were extracted from the WRF output and stored in the database for further application in the screening regression procedure. Table A.1 in Appendix A summarizes information about the predictors.

4.5.5.3 Building the MOS model

MOS models were built separately for the two locations (HOPE and AGASSIZ) and for two seasons. The summer season covers 6 months, April–September, and the winter season includes 6 months, October–March. The available 3 years

(2007, 2008, 2009) of WRF simulations were divided so that the data for 2007 and 2008 were used to build the MOS model (dependent dataset), and the simulations for 2009 were applied for validation purposes (independent dataset). Tables A.2, A.3, and A.4 in Appendix A present coefficients of the regression equations of ambient temperature, wind speed, and wind direction respectively.

4.5.5.4 Ampacity calculation

To estimate how the improvement in numerical weather simulations affects calculations of the thermal rating, a series of ampacities was calculated. Three datasets of weather parameters were applied: (1) raw output from the numerical model, (2) weather predictions of the numerical model improved with MOS, and (3) historical weather observations from the meteorological weather stations. The ampacity was calculated only for an independent dataset of 2009. The angle of line span headings was assumed to be 0 degrees, so that the line is directed from north to south.

4.5.6 Analysis of the results

Table 4.2 presents the main statistics – bias, mean absolute error (MAE), root-mean-square error (RMSE) – of the weather parameters – ambient temperature (T), wind speed (WSpd), wind direction (WDir)– simulated by the NWP model. The WRF column gives statistics for the raw output of the model, while the MOS column gives statistics for the postprocessed weather parameters. The analysis was performed by comparing actual weather observations at the weather stations (AGASSIZ and HOPE) with WRF weather predictions and MOS results.

The last two columns show the percentage of error reduction after MOS technique was applied. The results clearly demonstrate an improvement in weather parameter accuracy after MOS application. MOS removes the bias of the WRF model and significantly reduces the errors. The only exception is the bias of wind

AGASSIZ									
Variables	Season	BIAS		MAE		RMSE		MAE improved %	RMSE improved %
		WRF	MOS	WRF	MOS	WRF	MOS		
T, °C	winter	-0.09	0.05	2.3	1.79	2.88	2.28	22.40%	20.71%
	summer	-2.04	-0.65	2.84	1.56	3.56	1.98	45.12%	44.23%
WSpd, m/s	winter	1.67	-0.23	2.72	1.53	3.51	2.35	43.60%	33.08%
	summer	1.47	0.02	1.76	0.72	2.3	1.04	58.81%	54.74%
WDir, °	winter	-12.14	1.08	26.69	19.32	32.96	23.69	27.61%	28.14%
	summer	-9.52	1.63	27.15	20.88	33.96	24.96	23.10%	26.50%
HOPE									
T, °C	winter	0.47	0.24	2.64	1.85	3.35	2.39	29.66%	28.67%
	summer	-1.61	-0.26	2.43	1.56	3.17	2.06	35.95%	35.04%
WSpd, m/s	winter	0.63	0.19	2.25	1.62	3.08	2.04	28.04%	33.87%
	summer	2.25	0.28	2.89	1.27	3.67	1.62	55.97%	55.89%
WDir, °	winter	0.21	7.08	24.92	17.75	33.02	26.43	28.75%	19.94%
	summer	5.43	7.9	24.01	19.77	31.85	28.46	17.66%	10.64%

Table 4.2: Summary statistics of NWP weather simulations before and after MOS application.

direction at the HOPE weather station, which was increased. The most extensive improvements are observed for wind speed, and this is especially beneficial for thermal rating calculations. For instance, the MAE of wind speed at the AGASSIZ weather station during the summer season, 1.76 m/s, was reduced to 0.72 m/s after MOS treatment, an error reduction of almost 60 %.

Improvement in the accuracy of weather conditions can also be shown in the time-series where data from three datasets are presented (WRF raw output, WRF data improved with MOS, and weather observations recorded at the weather stations). Figure 4.8 and Figure 4.9 show the time-series data of temperature and wind speed for June 2, 2009. It can be seen that the MOS data (improved weather variables) are much closer to the values of actual weather parameters observed at the weather stations. This is especially noticeable in the graphic of wind speed. Air temperature is originally predicted well by the WRF model, and the reduction of error in not as evident as for wind speed.

Clearly, weather parameters simulated by the WRF model were significantly improved using MOS. The next step was to estimate how these improvements af-

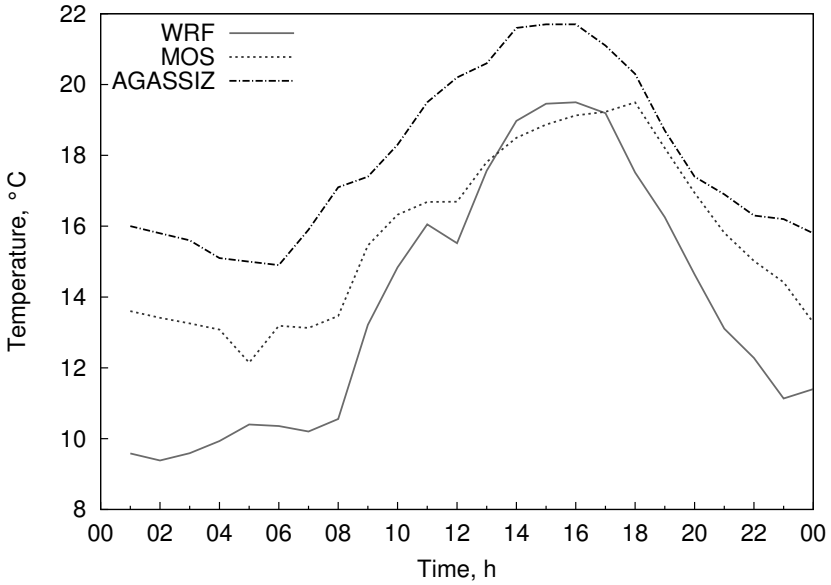

Figure 4.8: Comparison of three datasets of ambient temperature: simulated by WRF, improved with MOS, and observed at the AGASSIZ weather station (June 7, 2009).

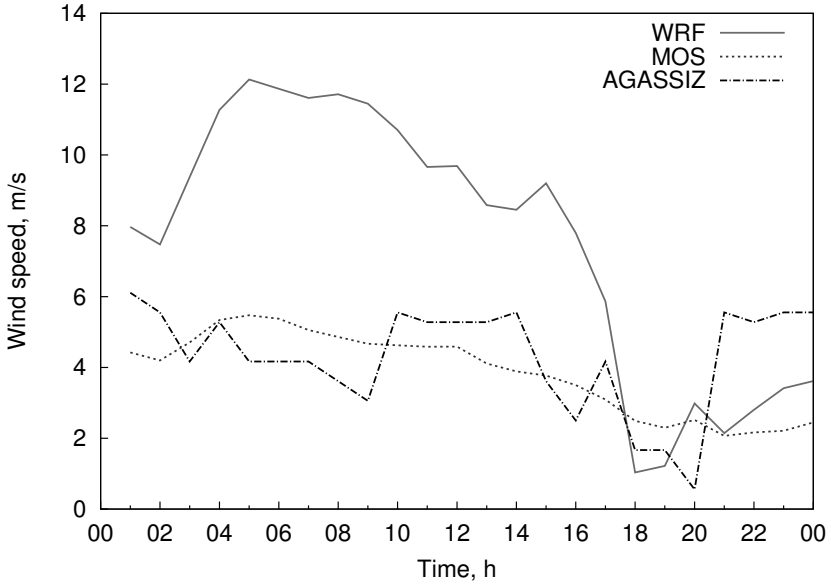

Figure 4.9: Comparison of three datasets of wind speed: simulated by WRF, improved with MOS, and observed at the AGASSIZ weather station (June 1, 2009).

fect DTR calculations. For this purpose, thermal rating was calculated again using three independent datasets (WRF raw output, MOS results, and actual weather observations from the weather stations). Ampacity calculated based on histori-

cal weather data (data from the weather stations) was considered as "true" line ampacity. DTR results obtained with WRF and WRF-MOS weather data were compared to the desired "true" ampacity. The main estimation statistics are presented in Table 4.3, which also contains analysis results for conductor temperature. As conductor temperature is one of the important safety parameters of a power line, it is useful to estimate the impact of MOS on line temperature predictions, therefore, conductor temperature was calculated in addition to ampacity. It was assumed that the line was fully loaded under two different dynamic thermal rating calculations (WRF and WRF-MOS), while ambient weather conditions remained as they were observed at the weather stations. Such a scenario imitates the actual application of the DTR-NWP system.

AGASSIZ								
Variables	BIAS		MAE		RMSE		MAE improved %	RMSE improved %
	WRF	MOS	WRF	MOS	WRF	MOS		
Ampacity, A	149	68	287	212	360	272	26.04%	24.37%
Line temperature, °C	55	45	58	45	75	53	22.59%	28.90%
HOPE								
Ampacity, A	156	96	355	236	444	318	33.54%	28.51%
Line temperature, °C	63	54	67	55	82	61	18.53%	26.52%

Table 4.3: Summary statistics of ampacity and conductor temperature calculations based on raw WRF data and improved MOS data.

The results in Table 4.3 demonstrate that both ampacity and conductor temperature calculations were significantly improved using MOS. As the biases of conductor temperature and ampacity are positive values, they are consistently overestimated. This undesirable behaviour requires further investigation.

Figure 4.10 shows time-series of ampacities calculated using different datasets of weather parameters. The dynamic thermal rating improved with MOS are closer to the actual line ampacity than the rating obtained with raw WRF output.

Table 4.4 shows the percentage of time the line is overheated under the two DTRs. It can be seen that after MOS treatment (DTR-MOS) there was signif-

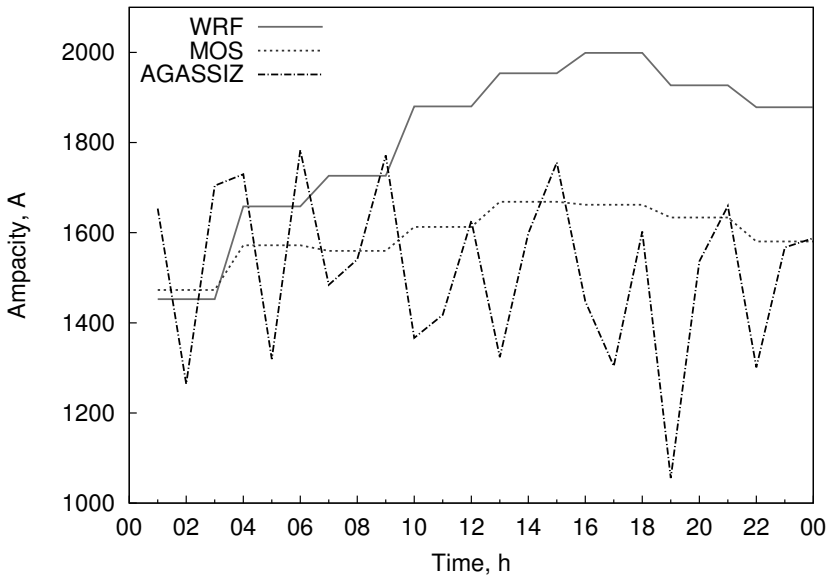

Figure 4.10: Comparison of three dynamic thermal ratings: DTR-WRF, DTR-MOS, and actual ampacity (June 1, 2009).

icantly less line overheating than the before MOS treatment (DTR-WRF). The most substantial improvement is observed for the higher conductor temperatures (temperatures $> 95\,^{\circ}\mathrm{C}$ and $> 150\,^{\circ}\mathrm{C}$), where it is most required.

	Percentage of time in temperature range			
	$75\,^{\circ}\mathrm{C} < t \leq 95\,^{\circ}\mathrm{C}$	$95\,^{\circ}\mathrm{C} < t \leq 150\,^{\circ}\mathrm{C}$	$t > 150\,^{\circ}\mathrm{C}$	$t \leq 75\,^{\circ}\mathrm{C}$
DTR-WRF	66.60%	49.00%	15.50%	33.40%
DTR-MOS	61.30%	39.10%	6.20%	38.70%
Improvement %	8.00%	20.10%	60.10%	13.80%

Table 4.4: Percentage of time the conductor is overheated under DTR-WRF and DTR-MOS.

In the MOS study, ampacities were calculated based on weather data from two separate locations (weather stations in AGASSIZ and HOPE) situated in close proximity to power transmission line 5L081. Weather parameters from the stations were used to calculate a dynamic thermal rating of the line. Table 4.5 summarizes the results of different ampacity estimations. The table contains values of average ampacity of two line spans located at the weather stations. Ampacities calculated based on WRF weather data, WRF simulations improved with MOS,

and actual weather observations are given in Table 4.5. The average ampacity of the transmission line is based only on the WRF predictions, as the MOS model wasnt tested for all line spans, and it is not possible to estimate the "true" line ampacity without actual weather observations at each line span.

	Average ampacity, A		
	DTR-WRF	DTR-MOS	"True" Ampacity
5L081	983		
AGASSIZ	1387	1322	1201
HOPE	1729	1682	1461

Table 4.5: Average ampacity calculated for a segment of transmission line 5L081 and two line spans located at weather stations in AGASSIZ and HOPE.

A comparison of different average ampacities demonstrates that the actual rating of the line is significantly lower than the ratings of two separate line spans. The rating of the line is based on the weather conditions along all line spans, and hot spots (the span with the lowest ampacity) in the line that change position. The line rating is based on the worst weather conditions that occur along the transmission corridor, while the span rating cannot guarantee that the weather parameters at the location of that span are the worst.

Based on the results, it is possible to conclude that even without error reduction of the WRF simulations, DTR-NWP produces more reliable and safer dynamic thermal rating than the dynamic thermal rating obtained based on the weather observations from just a few spots along the line.

4.6 Summary

This chapter presents the theoretical background of MOS and reviews the main principles of MOS application for improvement of DTR-NWP calculations. It was shown that the accuracy of the numerical weather simulations for the purpose of dynamic thermal rating calculations must be considered differently from the

accuracy of regular weather forecasts. For DTR, weather parameters are counted as critical errors only if they raise the rating higher than the actual line ampacity and can thus lead to violation of the thermal limit. The MOS procedure requires historical weather observations for building regression equations. All available weather parameters are analysed and potential sources of error are identified.

A case study was performed to examine the utility of applying MOS to DTR-WRF calculations. It was shown that errors in numerical simulations of ambient temperature, wind speed, and wind direction can be significantly reduced by post-processing raw NWP output with MOS regression equations; up to nearly 60 % error reduction was observed. MOS removes the bias of the NWP model and substantially decreases MAE and RMSE of weather simulations. Improvement in numerical weather prediction leads to improvement in DTR calculations. Results of the ampacity calculations performed for two different locations (AGASSIZ and HOPE weather stations) demonstrated that the WRF data improved with the MOS procedure and errors in rating estimations were reduced. Occurrences of conductor overheating were also reduced when MOS were applied, especially for cases where conductor temperature rose above 95 °C. Comparison of ampacity calculations performed for sample line 5L081 and for two assumed line spans showed that the rating of a single span is significantly higher than the rating of a line. Therefore, DTR based on numerical weather simulations is more reliable and safer than methods based on the weather observations from remote weather stations, as the former considers the worst case weather conditions along all spans of the line.

Chapter 5

Information Technologies in the DTR System

The amount of data produced by the Advanced Dynamic Thermal Rating (DTR) system based on the Numerical Weather Prediction (NWP) model can easily reach several terabytes, depending on the temporal and spatial resolution of weather simulations and the length of the transmission line. For efficient data manipulation, information must be well structured and organized. Relational databases together with data historians form the backbone of data storage and management. Integration of the NWP model into the DTR system requires the development of new database schemas, programming interfaces, and user-friendly client-side applications. Another important aspect of the DTR system is data visualization. Calculated ampacity and ambient weather conditions must be presented graphically with map overlays. Web-based technologies bring new possibilities to share information among stakeholders more easily and efficiently [53]. 3D visualization of the transmission assets together with interactive graphics can benefit system operators and maintenance crews, and interaction capabilities can simplify data analysis and help users to understand the current state of the transmission system.

5.1 Database organization

This section describes a database schema to support data generated by the DTR system. Two datasets that must be stored in the database are the input parameters of the calculation algorithms and the output parameters produced by the system. Input parameters are numerical weather simulations, physical characteristics of the conductor, and geographical attributes of the transmission lines. Output parameters are the calculated thermal rating, conductor temperature, line sag, and accumulated loss of conductor strength.

The amount of data produced by the DTR system depends on the spatial and temporal resolution of the calculations. It can easily reach several terabytes, and efficiency of data storage and retrieval will depend on data organization. A relational database management system (RDBMS) is a well-proven solution to data storage. Saving output from the DTR system into a relational database will assure consistency and reliability of the data and simplify data processing and analysis significantly. An RDBMS can be integrated into the work flow of an electric utility company and interconnected with existing information systems [54].

It is important to preserve the spatial context of parameters produced by the DTR system such as line ampacity and weather conditions. Therefore, it is important that the RDBMS can support geographic types of data such as polylines and polygons. The PostgreSQL RDBMS was chosen for the data storage in this project. PostgreSQL is open source software that is being actively developed, and demonstrates high performance in data manipulation [55]. The RDBMS contains a powerful geospatial module PostGIS, which provides support for geographic objects. PostgreSQL with PostGIS installed is a spatial database capable of storing and operating georeferenced data. PostGIS possesses quite a wide functionality: coordinate transformation, geospatial measurements, detection of geometries interaction, etc. It is supported by many geographic information systems (GIS) [56].

Development of a new database structure for the DTR system must follow the basic principles of relational databases. First of all, data duplication in the database must be avoided. For example, a circuit name must be saved just once in the data table. If another table needs to refer to a particular circuit, it will use a foreign key (an identification number of the record in another table). In such case, information should be referenced, but not copied. Data modification takes place in one table only, and all the connections among entities remain valid. Foreign keys constrain the data, assuring data consistency through a child-parent connection between tables. Another advantage of such a design is that the data logic is concentrated at the database level. Development of new software that uses data from the database will be significantly simplified.

Database organization includes the development of a database schema and integration of the database into the DTR system. The following two subsections cover the corresponding topics.

5.1.1 Entities

The database schema for the DTR system can be described by several tables, which are also called entities. The tables can be divided into three closely connected logical groups: "transmission system, " "calculations," and "meteorological observations." The entity relationship diagram is presented in Figure 5.1.

5.1.1.1 "Transmission system"

Tables of the "transmission system" group describe only the most important components of a power transmission system. Other tables, not covered in this discussion, may include information about system inventories, inspections, and asset conditions, and more parameters can be included in the proposed tables (e.g., line voltage; type, style, and height of towers), but additional tables and data fields will not change the database schema.

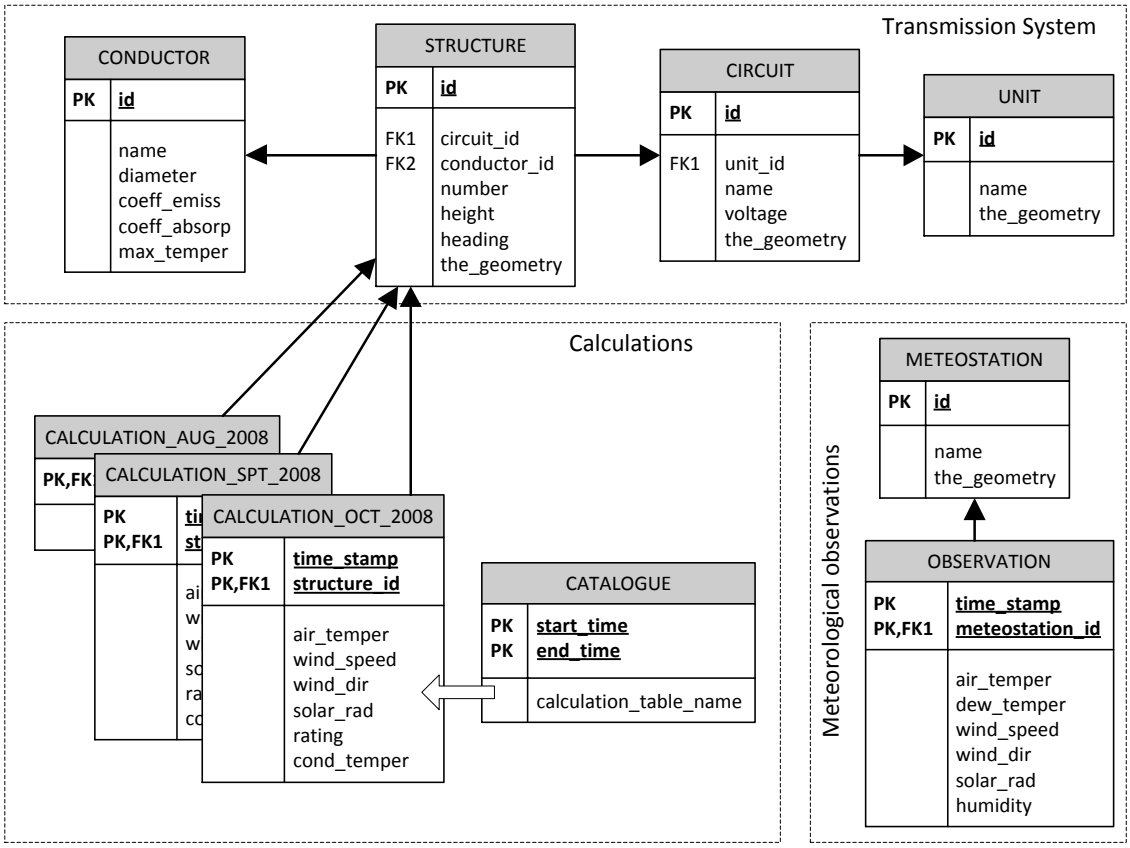

Figure 5.1: Model of the database of the DTR system.

In many cases, transmission circuits are grouped together by their geographical locations into units described by the table `UNIT`. Power lines are included in the table `CIRCUIT`, and the power structures are shown in the entity STRUCTURE. The conductor type information is stored in a separate table – `CONDUCTOR`. It is assumed that each structure also represents the following span of the line, so that for each span, the conductor description will be accessible through the foreign key `conductor_id`, and all the calculations (ampacity, conductor temperature, etc.) will be connected to a particular line span. There is a potential data inconsistency for the last tower of the line; if it is the ending structure, there is no further span. In this case, `conductor_id` will be equal to NULL, and the query will return NULL instead of the conductor type.

Circuits, structures, and units contain geographical information saved in in

the field `the_geometry` of each table. Typically, two numerical columns, latitude and longitude, would be sufficient to describe the location of each transmission tower, but for storing lines and polygons a special geographical type is required – the PostGIS geometry type. This type is used for all georeferenced data. Also, PostGIS provides plenty of functions to manage and analyze GIS objects of the type geometry (e.g., functions of spatial relationship and measurements, geometry processing, linear referencing). The additional spatial field heading in the table `STRUCTURE` holds the bearing of each line span, which is used for ampacity/temperature calculations and correct visualization of the transmission structures.

5.1.1.2 "Calculations"

Output from the DTR system (ampacity, conductor temperature, conductor sag, etc.) is stored in the tables `CALCULATION_[MONTH]_[YEAR]`. Several tables with the same structure are required because the number of rows can easily reach tens of millions. For example, if the data are stored every ten minutes for a single transmission line with 200 towers for a period of one year, there will be about 10.5 million rows. Such a large number of rows can reduce the efficiency of queries and data analysis. Therefore, logical separation of calculations is necessary. The table `CATALOGUE` is included to speed up finding the calculation tables based on a specified period of time. The tables `CATALOGUE` and `CALCULATION_[MONTH]_[YEAR]` are not strongly connected through the primary foreign keys mechanism, so triggers must be created to preserve data consistency.

5.1.1.3 "Meteorological observations"

The core of the DTR system is a numerical weather model; the actual weather observations from weather stations are necessary to validate the output of the model and build appropriate equations. A minimum of two tables – `METEOSTATION`

and `OBSERVATION` – is required to store meteorological observations in the DTR system database. Each weather observation is connected to a particular weather station through the `meteostation_id` key. The tables `METEOSTATION` and `UNIT` can be connected, so that it will be easy to aggregate available meteorological observations for an area of the system unit. Alternatively, the same results can be obtained with sql stored procedures and PostGIS functions.

5.1.2 Database in the DTR system

Figure 5.2 shows the main components of the DTR system and their connections with the database. The output from the NWP model (in form of NetCDF files) and the actual weather observations (in form of ASCII files) are directed to the Data Parser which extracts, organizes, and stores required weather parameters in the database. The Data Parser separates different data sources and various data formats from the other modules of the DTR system. As soon as weather conditions are stored in the database, other software modules will operate directly with the database. This guaranties uniform data flow. For example, the MOS and Ampacity/Temperature Calculator modules extract necessary information from the database, perform calculations, and return the processed data back to the database. Other system components (Analysis, Visualization, Rating Prediction, etc.) communicate with the data source similarly. It will be shown in the following subsections that such system organization is very efficient and provides great flexibility for software development and system integration.

5.2 Web-based interactive graphics and maps

The importance of data visualization for the DTR system is outlined in the introduction to the current chapter. This section describes the methodology of presenting a DTR system's data in the form of Web-based interactive graphics

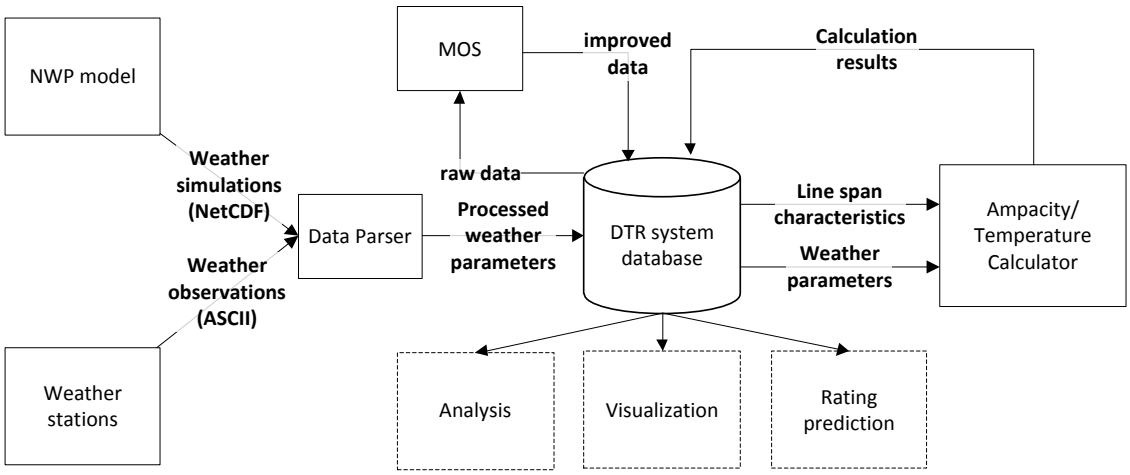

Figure 5.2: Modules of the DTR system.

and maps.

The ability to access data through a Web browser allows users to avoid complexities of software installation and additional configuration processes [57]. The back-end logic is implemented on the server side, and the data are fed from the DTR systems database. A Web-based approach simplifies access to the data and ensures that the most recent calculations are available to all users simultaneously.

Most data stored in the database (e.g. weather simulations, calculated ampacity and conductor temperature, transmission system assets) contain geospatial content and must be presented on a geographic map. The ability to zoom to a particular location, pan the map, and interact with the data helps a decision maker to understand the conditions of the transmission system and to solve problems more efficiently. The Google Earth Plug-in (GEPlugin) is proposed as a GIS visualization platform for the DTR system. The GEPlugin presents the same 3D virtual globe as the GE desktop application, but in a Web browser. The functionality of the GE extension is controlled through its application programming interface (API), which is a JavaScript library with a variety of objects and functions. The library is located on Google servers and is accessed by linking to it through HTML code. An Internet connection is required to launch GEPlugin, however, after it is

loaded by a Web browser, it works similarly to the GE desktop application if the Internet connection is broken.

DTR system data in the form of interactive plots and graphics are implemented with Google Chart Tools. The Tools provide plots, charts, and graphics that can be integrated into a Web page. The graphics allow a user to navigate through the data, investigate the trends, and compare several data series simultaneously. The main programming language of the library is JavaScript, and data from a remote source are extracted by a hypertext transfer protocol (HTTP) request. The same principle is used to present the data from the DTR systems database in GEPlugin. The next subsections describe how the data from the DTR system can be visualized with Google technologies.

5.2.1 Geospatial visualization

Transmission lines, individual towers, weather conditions, and calculated line ampacity/temperature can be effectively presented on a 3D map in GEPlugin. The main components of the visualization module are presented in Figure 5.3.

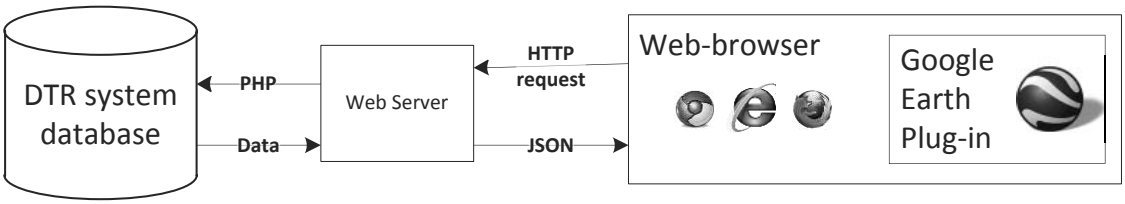

Figure 5.3: Visualization module of the DTR system.

Initially, a Web browser sends an HTTP request to a Web server to launch a hypertext preprocessor (PHP) script. The Web server extracts the data from the database as plain text using PHP functions and encodes it in JavaScript object notation (JSON) format. Then the JSON string is sent back to the client, where it is decoded and the data are extracted into JavaScript objects. When the data from the database is on the client side, it can be visualized in GEPlugin.

The coordinates of transmission lines and individual towers, are retrieved from the DTR systems database using PostGIS functions. There are several possible output data formats, such as Keyhole Markup Language (KML), GeoJSON, and text. As the data are to be presented in GEPlugin, the KML format is preferable (KML is a native format for Google Earth). For the transmission lines, the returned KML type is `KmlMultiGeometry`; for the towers it is `KmlPoint`. Alternatively, the coordinates can be extracted from the database as a comma-separated text string and parsed into KML objects on the server side. This approach is more flexible as it allows data preprocessing before its conversion to a JSON string. The downside of the text format is that additional data parsing can significantly increase the time of data preparation.

Figure 5.4 demonstrates how BC Hydro power transmission lines stored in the database can be presented in GEPlugin. Additional parameters of the transmission lines such as voltage, name, and description are extracted from the database along with the coordinates. For example, line color is assigned based on line voltage (500 kV–red, 230 kV–green, 69 kV–black).

Weather parameters produced by the NWP model of the DTR system are visualized using an approach similar to visualization of the transmission lines. The required data are extracted from the database through an HTTP request to the Web server, then, on the client side, weather parameters are transferred into coloured graphical primitives – so-called KML placemarks. The wind direction at each line span is depicted as an arrow icon, and the temperature is shown as a circle. The wind speed icons are scaled to demonstrate the relative magnitude of wind velocity and the arrows point in the direction of the wind. The placemarks representing ambient temperature are coloured according to temperature values. The colour gradually changes from blue to red depending on how close the actual temperature is to the minimum or maximum temperature, respectively (Figure 5.5).

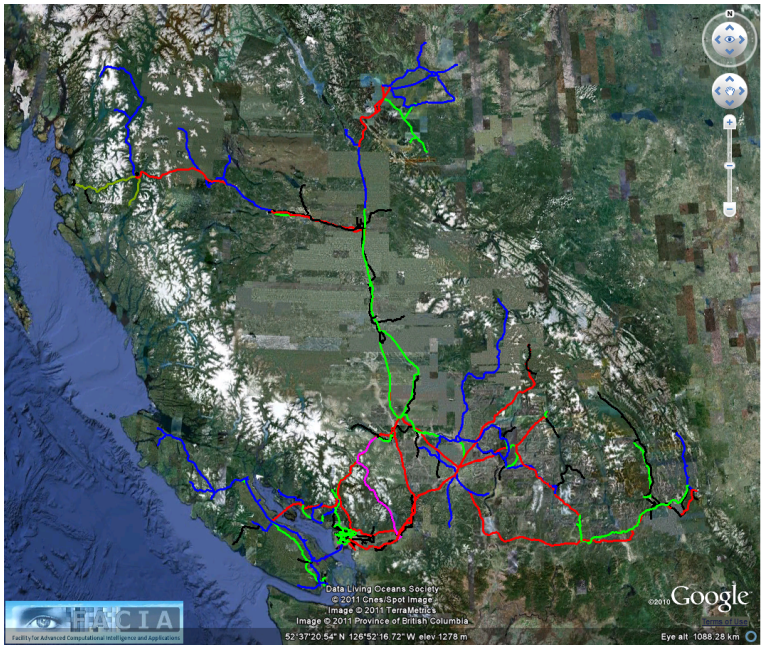

Figure 5.4: Visualization of the BC Hydro power transmission lines.

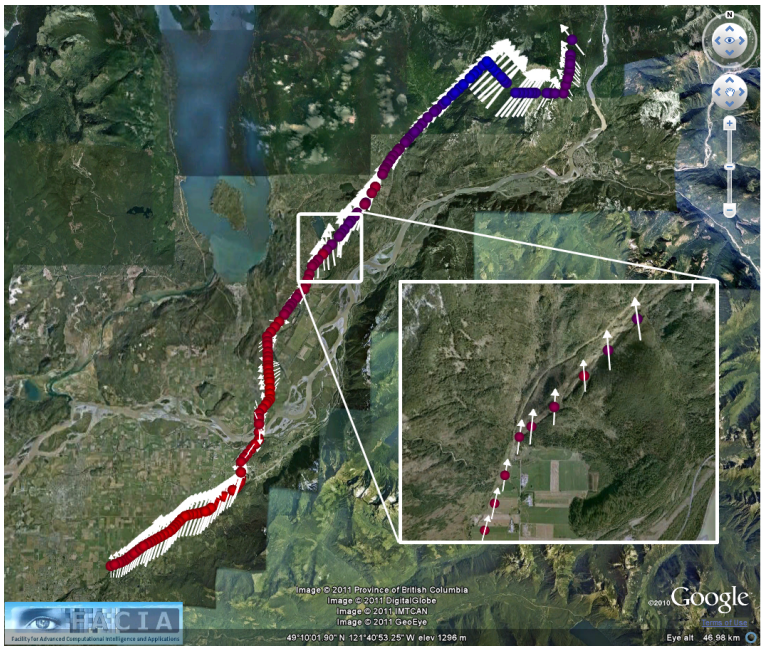

Figure 5.5: Visualization of weather parameters (wind speed, wind direction, and air temperature) along a section of the BC Hydro power transmission line 5L081 (July 01, 2007, 14:00).

The calculated dynamic ampacity is also presented as a map overlay in GEPlugin (Figure 5.6). Similar to ambient temperature, the dynamic ampacity at

each line span is represented by a coloured circle: green for relatively high and red for relatively low values of ampacity. Simultaneous visualization of several data layers on a map can give a system operator new insights about the state of the transmission system. For example, visualization of wind characteristics together with dynamic ampacity demonstrates the relationship between wind direction, wind speed, and dynamic rating values (Figure 5.6).

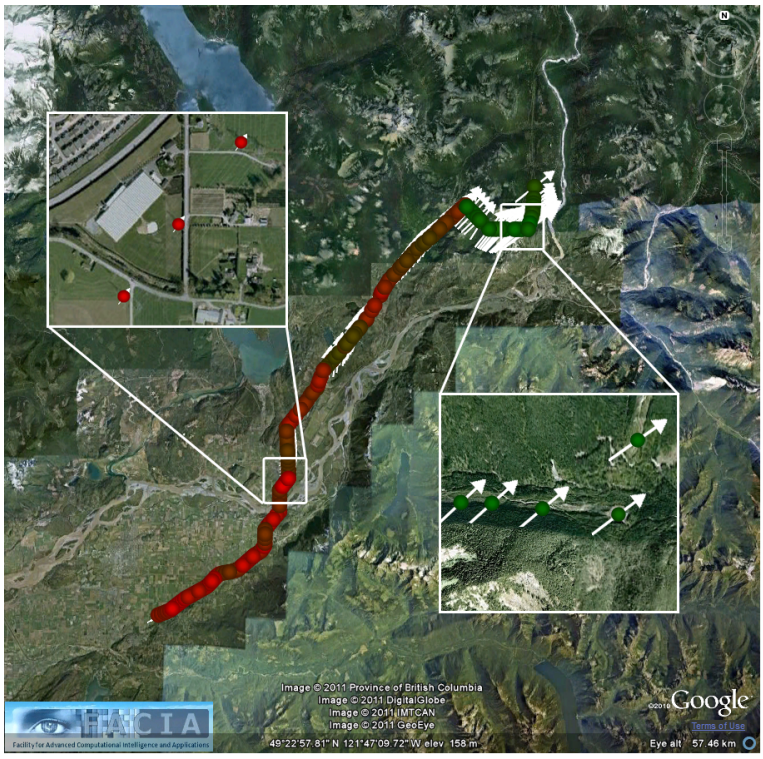

Figure 5.6: Visualization of the dynamic ampacity calculated for each line span of a section of the BC Hydro power transmission line 5L081 (July 01, 2007, 14:30).

In Figure 5.6 it is seen that the ampacity is higher (dark circles) for line spans where the wind speed is high. It is also possible to determine the impact of the the angle of incidence of the wind. Wind blowing parallel to the conductor does not cool the line, and the dynamic thermal rating is low (light circles).

5.2.2 Interactive plots

Besides geospatial visualization, it is important to present the output from the DTR system in form of interactive graphics and plots, so it is easy to evaluate changes in the system. Time series plots demonstrate how the DTR systems calculations are altering in time. Spatial distribution of a parameter can be presented with static (snapshot) graphics. Google Chart Tools provide two types of graphics, Annotated Time Line and Line Chart.

The use of Annotated Time Line is presented in Figure 5.7. The graphic shows the air temperature (T2) simulated by the numerical model (WRF), the temperature observed at the Environment Canada weather station (EC), and the model temperature improved with the model output statistics technique (MOS). Valuable observations can be made from the plot. For example, it is seen that the

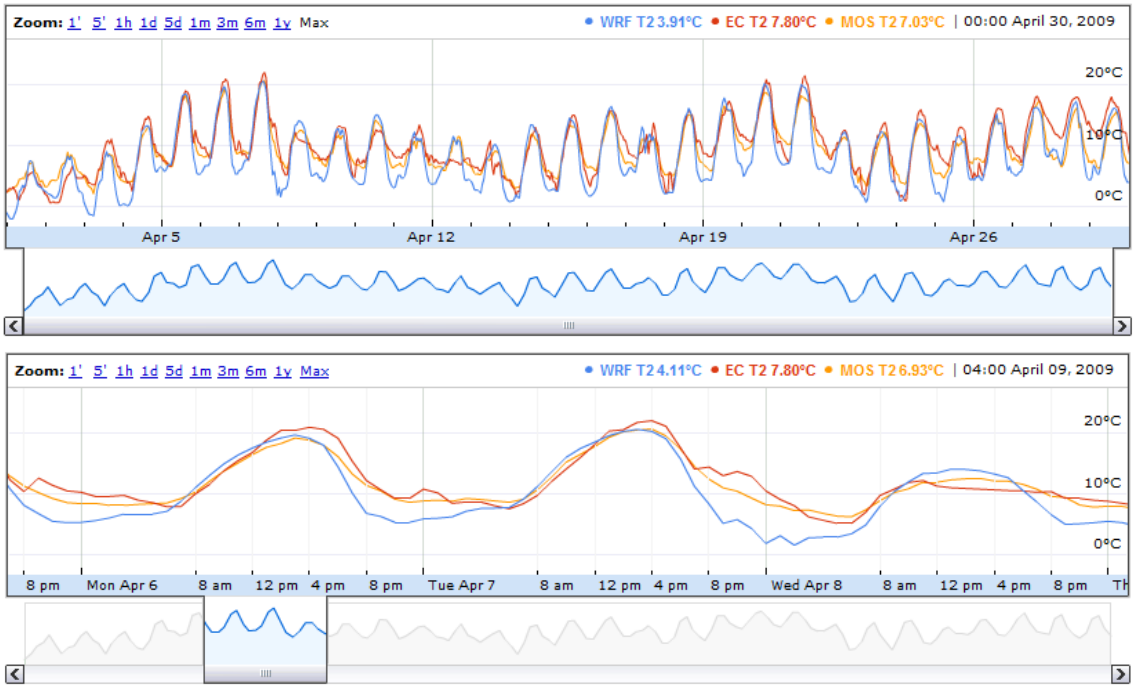

Figure 5.7: Time series graphic of the ambient temperature near tower #100 of the BC Hydro power transmission line 5L081 (top graphic: time resolution – one month, bottom graphic: time resolution–8 hours).

NWP model is very close to the actual ambient temperature during the daytime, but it produces a significant error during night hours. Such information helps the user to adjust the parameters of the NWP model to reduce simulation errors.

Line Chart is a static plot suitable for presenting spatially distributed data. Figure 5.8 demonstrates the distribution of dynamic ampacity along 155 spans of the power transmission line. Line Chart graphics do not provide the zooming and panning functionality of Annotated Time Line. However, it is possible to connect the plot with the GEPlugin map and investigate how weather conditions affect the thermal rating of a chosen line span .

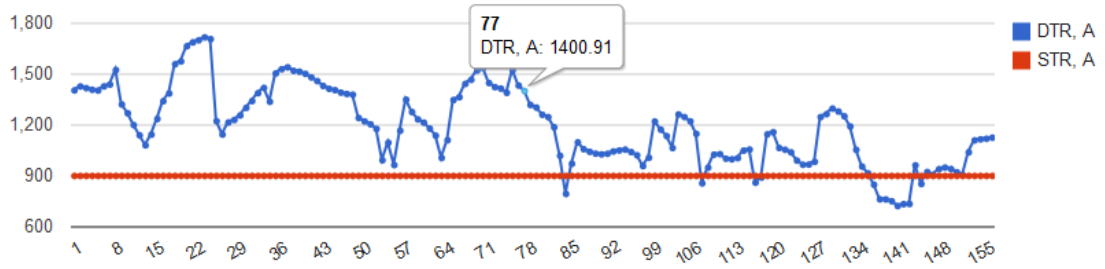

Figure 5.8: Visualization of the dynamic ampacity along a section of the BC Hydro transmission line 5L081 (July 01 , 2007, 11:00).

5.3 3D visualization of the transmission system assets

Presenting geospatial data in a form of 2D digital maps was a breakthrough in the 1980s. Since then, computer technologies have improved significantly, and yesterdays 2D maps are gradually evolving into todays 3D virtual world. 3D visualization is not a new information technology, but only modern computational power and innovative software technologies have enabled the building of immersive, highly visual 3D environments that can be integrated into workflows of various industries.

The electric transmission industry can benefit significantly from the use of 3D technologies. A 3D visualization of assets allows a system operator to know the exact location of the grid components and their alignment with surrounding objects such as trees, roads, and buildings. Important characteristics of power lines such as conductor sag, ground clearance, and height of the transmission structures can be visualized more clearly in a 3D environment compared to a conventional 2D map (Figure 5.9). The 3D advantage can increase the efficiency of power system operation and reduce the time of decision making.

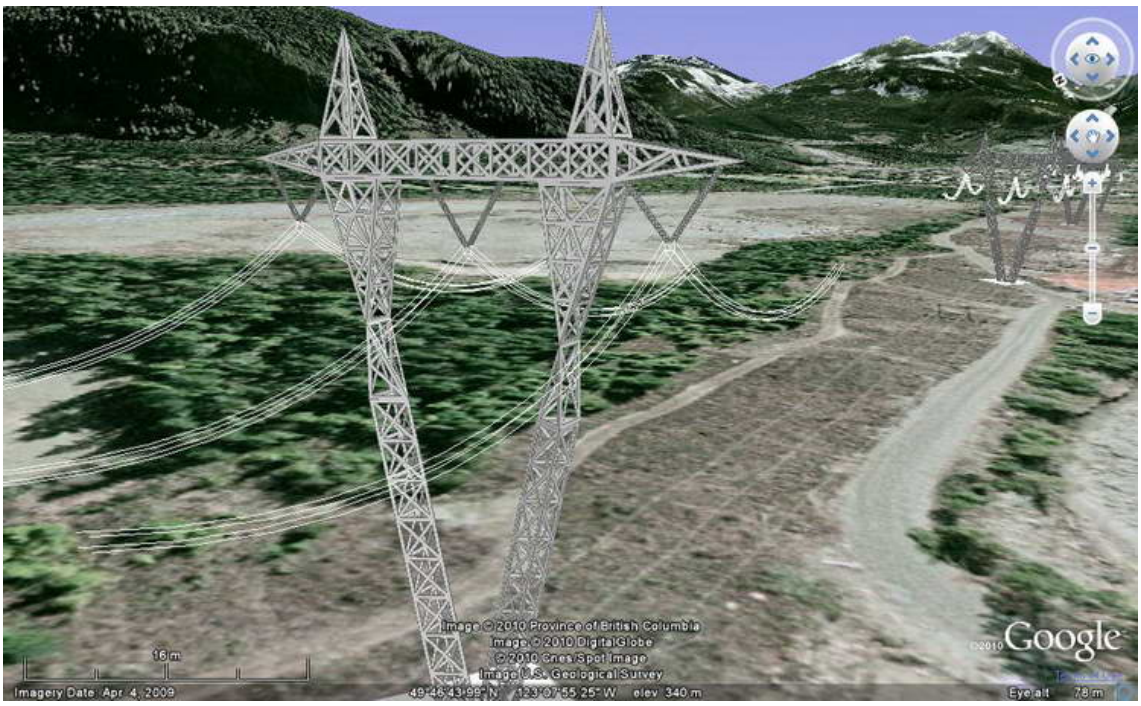

Figure 5.9: 3D visualization of the transmission system assets.

Modern 3D geographic visualization technologies are still young and not yet well adopted by the electric transmission industry. A number of software products and frameworks provide 3D visualization capabilities and can be used to enhance the graphical presentation of power transmission components: Google Earth, Microsoft Bing Maps 3D (formerly Virtual Earth), NASA World Wind, Oracle Spatial 3D, ESRI ArcGIS 3D Analyst, Intergraph GeoMedia 3D, and Autodesk AutoCAD Map 3D. Each of these technologies has pros and cons, and must be considered

based on the specific requirements of the electric utility. For the current research, Google Earth was chosen as the implementation platform.

The 3D environment of the Google Earth visualization system requires appropriate user-computer interaction methods. In the scope of the research, the possibilities of an advanced user control device, 3DConnexion SpacePilot Pro, were investigated. The main advantage of this joystick-like device is that it provides flexible and intuitive navigation in a 3D environment. In contrast to a traditional mouse, complex movements in several directions can be performed simultaneously. Flying over transmission lines, zooming in to a particular transmission structure, or investigating the details of the terrain is easy and intuitive with SpacePilot Pro.

5.3.1 System design

Similar to geospatial visualization, the core of the 3D visualization system is the Google Earth Plug-in. Today, there are several platforms for presenting geospatial data in 3D; Google Earth is one of the most efficient, user-friendly, and flexible solutions. Other 3D visualization frameworks (e.g., Oracle Spatial 3D and ESRI ArcGIS 3D Analyst) have their own benefits and could be considered for future projects.

The 3D visualization system was built using the capabilities of Microsofts .NET Framework. Two main libraries of the framework were usedWindows Forms and ADO.NET. Windows Forms provides graphical components for creating a robust and efficient graphical user interface. ADO.NET is used for implementing database interaction. GEPlugin was integrated into the program through a Web browser object, part of the Windows Forms library. Connection to the DTR system database was realized with ADO.NET. C# was the main programming language in the development process. A prototype of the system's graphical user interface (GUI) is presented in Figure 5.10.

For presenting transmission system structures in 3D, a library of 3D models

Figure 5.10: Graphical user interface of the 3D visualization system.

was created, covering the most widely used structures. Google SketchUp was used to construct 3D objects of the steel towers and wooden poles. Information about a particular structure, retrieved from the database, includes the structure type. Based on the type, an appropriate model is selected for visualization. Besides location information, each tower in the database contains information about the line span heading so it is possible to position the models correctly.

The architecture of the 3D visualization system was designed in such a way that program functionality was easily extended and improved. Database connection, visualization, and graphical user interface were separated into different modules. The advantage of such an approach is that changes in one module will not affect the entire program. For example, if the database is changed, only the corresponding module will require adjustments. Similarly, if the graphical user interface needs to be modified, this will not influence the functionality of the entire system.

To integrate SpacePilot Pro into the visualization system, the algorithms of earth rotation, panning, zooming, and tilting were implemented. The algorithms

are based on coordinate system transformation and vector rotation operations.

The created 3D visualization system demonstrated several different information technologies and provided insight into how 3D visualization can benefit transmission system operation and electric utilities in general.

5.3.2 Implementation

The developed 3D visualization system contained three modulesdata interaction, visualization, and program logic (Figure 5.11). All modules contained a set of classes responsible for specific tasks.

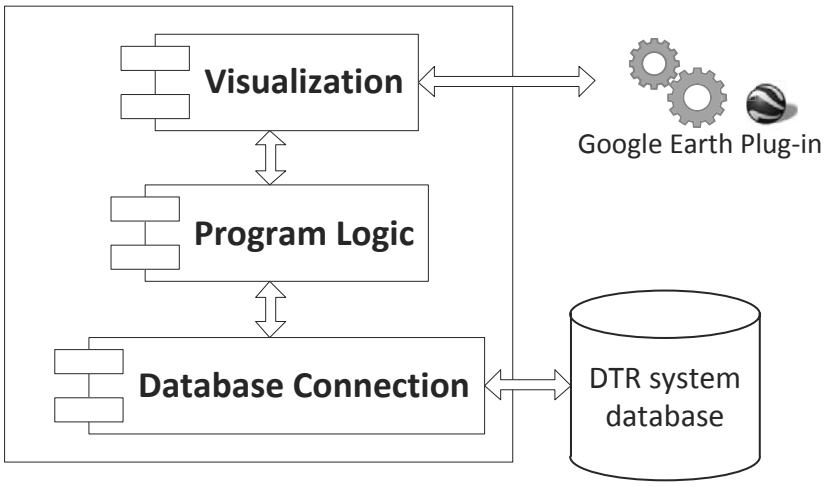

Figure 5.11: Main software components of the 3D visualization system.

5.3.2.1 Database Connection Module

ADO.NET was used to provide a read/write connection to the database. The DataSet class is one of the central objects in the ADO.NET library. It contains information about all database entities (in the form of DataTable objects) and entities relationships (in the form of DataRelation objects). The relationship among tables is supported by UniqueConstraint and ForeignKeyConstraint objects. These two types ensure the validity of tables primary and foreign keys, and help to control data in related (child) tables. The objects mentioned above

represent the static database organization inside the program. Another important class of the ADO.NET library, TableAdapter, provides data communication between the application and the database. TableAdapter objects are designed for each table in the database. The main task of these objects is to execute queries or stored procedures, and to return the data to the application (to fill DataSet). TableAdapter also sends the updated data (from DataSet) back to the database. Each TableAdapter object holds information about the data provider – the underlying data source. In this project, ODBC .NET Data Provider was used. A simplified class diagram of the Database Connection module is presented in Figure 5.12. A complete class diagram can be generated from the source code by means of Visual Studio.

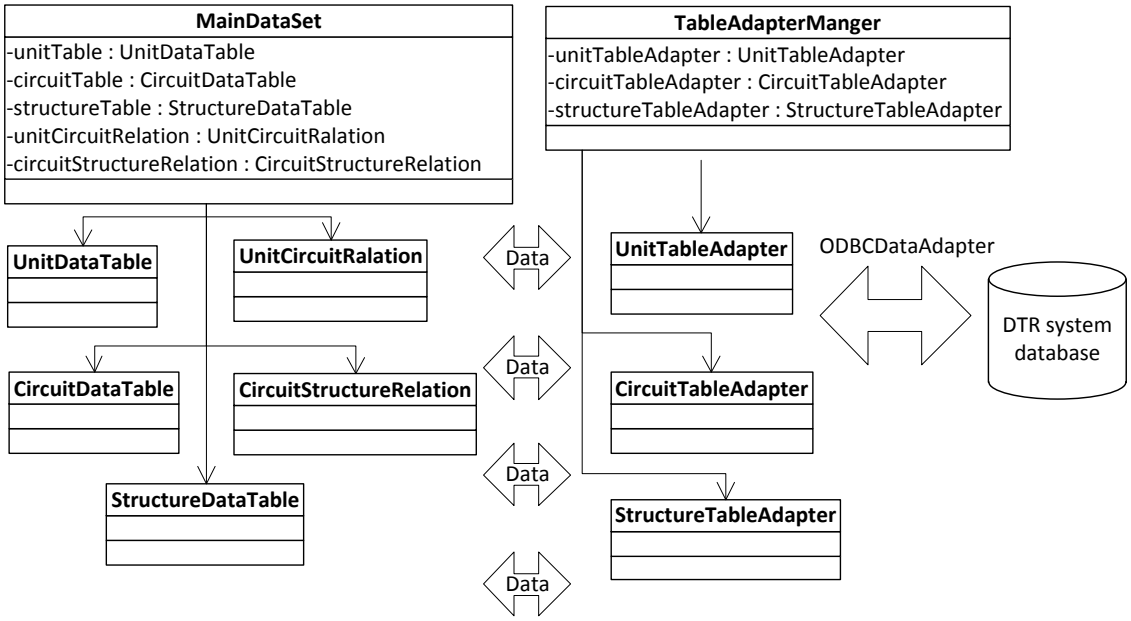

Figure 5.12: Main classes of the Database Connection module.

5.3.2.2 Program Logic Module

The Program Logic module is responsible for processing the raw data obtained from the database, and organizing them as a set of well-defined representative objects. This program layer aims to separate visualization functionality from

actual data organization. Such approach simplifies application support and update. If the underlying data source is changed, e.g., from the PostgreSQL database to a set of KML files, the program logic will need only minor modifications. Similarly, if the visualization component is changed, e.g., from Google Earth to ESRI 3DAnalyst, this modification will not affect data organization.

The main class of the Program Logic module is TransmissionSystem. There is only one object of this class in the program; it represents the entire transmission system infrastructure in the program. TransmissionSystem contains a list of units (Unit objects), which is a root for other transmission system elementscircuits. Structure objects are accessible through Circuit objects. Besides structural organization, TransmissionSystem may contain information about system inspections (Inspection), inventories (Inventory), and work schedules (Schedule). The main classes of the Program Logic module are presented in Figure 5.13.

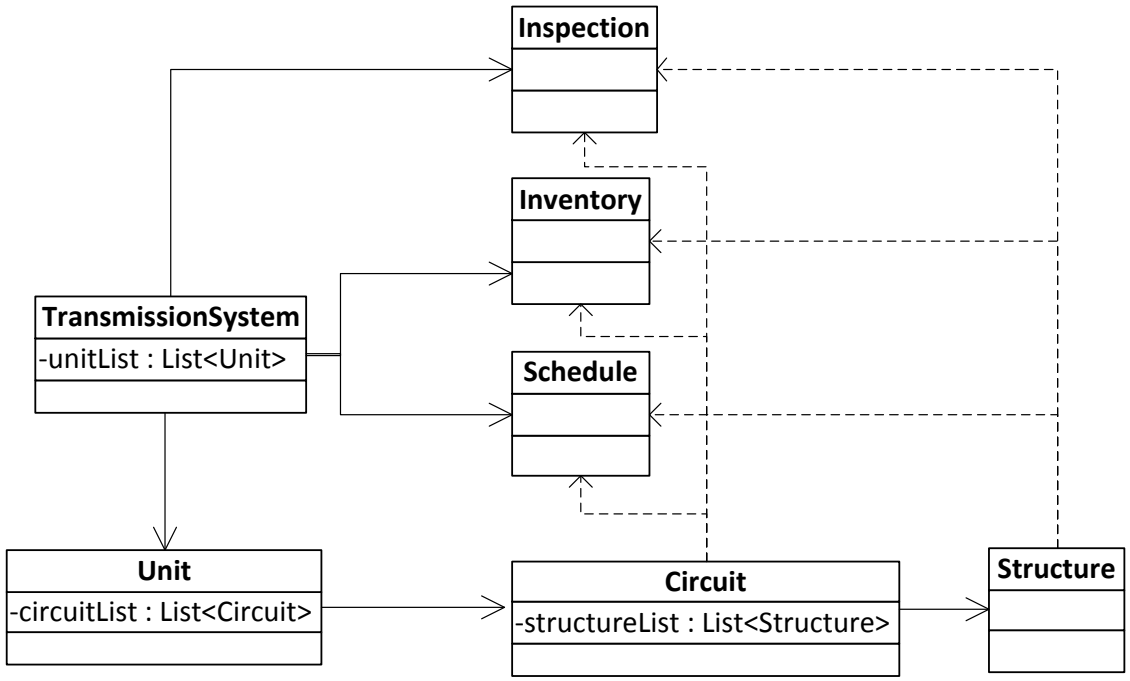

Figure 5.13: Main classes of the Program Logic module.

The TransmissionSystem object along with Unit objects and Circuit objects are created when the program starts. All other components are created when

needed. For example, a list of structures for a particular circuit is loaded only when the user requests such information. To load all the data from the database is not possible, due to the large amount of information involved. When the objects representing the transmission system are constructed and filled with data, they can be visualized in the Google Earth Plug-in.

5.3.2.3 Visualization Module

The Visualization module implements the visualization functionality of the application. The main component of this module is a GEWebBrowser class. This class is a part of the open source "winforms-geplugin-control-library." GEWebBrowser inherits a WebBrowser class from the Windows Forms library (.NET) and thus provides a complete functionality of a regular Web browser – a key requirement for using GEPlugin in a desktop application. Additional functions of GEWebBrowser simplify the creation of GEPlugin instances and process user events.

Another major class in the Visualization module is GoogleEarthViewer. It combines several auxiliary objects to control the style of the presented 3D models, filter selected objects, and process user events. User interaction events with the globe and with the 3D models first come to the GEWebBrowser object and then are redirected to GoogleEarthViewer. It is worth mentioning that GoogleEarthViewer is a bottleneck of the Visualization module. When more user interaction functionality is added to the program, GoogleEarthViewer will need to be refactored. A possible solution is to split GoogleEarthViewer into several classes responsible for specific user actions. Synchronization among different components can be implemented through the Event/Handler mechanism.

Another important function of GoogleEarthViewer is the rotation of the globe with the 3D mouse SpaceNavigator. The Google Earth API does not have a method to rotate the globe. The only possible way is to change the camera

view by specifying the coordinates of the camera and its three angles – heading, tilt, and roll. An algorithm for rotating an object around an arbitrary vector was implemented and integrated into the GoogleEarthViewer class. The signals coming from the SpaceNavigator are transformed into parameters of the camera view. Subsequently, the current view is refreshed.

GoogleEarthViewer creates 3D models based on information from the TransmissionSystem class. The access to graphical objects (IKmlObject, IKmlFeature, IKmlPlacemark, etc) is realized in GoogleEarthViewer, while all graphical components are physically saved in GEPlugin. A diagram of the major classes of the Visualization module is presented in Figure 5.14.

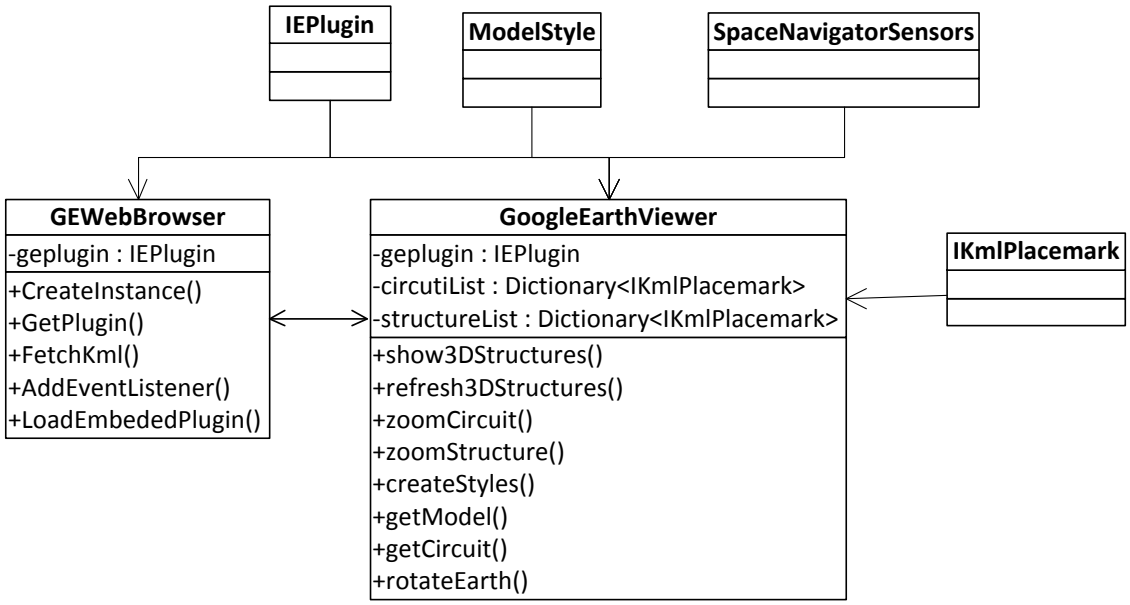

Figure 5.14: Main classes of the Visualization module.

Chapter 6

Conclusions, contributions, and future work

6.1 Conclusion

The capacity of transmission systems must be increased to cope with the growing demand for electricity and to support the development of clean generating stations working on renewable sources of energy. Straightforward solutions to this problem building new power transmission circuits or upgrading existing lines require large capital investments. A better approach is to increase the maximum electric current in the line through more accurate thermal rating. Uprating of a transmission line to gain extra current-carrying capacity can be a beneficial but hazardous step. Higher ratings allow electric utilities to transfer more energy, but increase the risk of line overload. Electric utilities should seek innovative thermal rating strategies that boost the efficiency and performance of the transmission system without endangering safety and reliability.

The research presented in the thesis examines and evaluates three advanced weather-based thermal rating approaches for high-voltage power transmission lines. The methods of thermal ratings reviewed include (1) seasonal probabilistic static

thermal rating, (2) probabilistic static rating based on data for a typical meteorological year, and (3) advanced dynamic thermal rating based on the NWP model.

6.2 Contributions

The results of evaluation of advanced weather-based thermal rating strategies show that probabilistic thermal ratings are generally higher than deterministic static ratings, as the former are based on observations of actual weather while the latter are based on conservative assumptions of ambient conditions. It was found that the transmission capacity of a transmission line operated under conventional STR was significantly underutilized; in one case study only 60 % of the potential current-carrying capacity was used. In contrast, seasonal STRs allowed line throughput up to 96 % of the estimated ampacity average. Seasonal STRs that change more frequently over a year, (e.g., STRf – 24 ratings for 12 months and day/night times) increased the average ampacity of the line more than seasonal STRs with fewer alternations (e.g., STRa – 1 rating over an entire year).

Results obtained for STRs based on weather data for a typical meteorological year (TMY) did not demonstrate as much capacity gain for transmission lines as seasonal ratings. STR-TMY (933 A) was 21 % higher than the conservative deterministic STR (729 A), and was 4 % higher than the nominal rating of the ACSR Drake conductor (900 A). The case studies for evaluating STR-TMY and seasonal STRs were performed in different geographical regions with different climatological zones and landscapes; thus, differences in the obtained results are not surprising.

Although advanced probabilistic STRs increase the current-carrying capacity of transmission lines, they also expose the lines to significant risks of thermal overload. For example, analysis of seasonal STRs showed that violation of the thermal limit (STR is higher than the actual ampacity) occurred 14 % to 20 % of the time, which is much higher than the risk tolerance level declared in the

calculations (5 %). The risks of thermal overload with STR-TMY were also underestimated, leading to violation of thermal limits and reduction in the reliability of the transmission system.

Another thermal rating approach studied in the research – advanced dynamic thermal rating based on a high-resolution NWP model (WRF) – did not display the shortcomings intrinsic to probabilistic ratings. DTR allowed monitoring of actual line ampacity in real time, accounting for changes in ambient weather conditions along the entire transmission corridor. Based on the calculated dynamic ampacities, utilities could operate a power system close to its thermal limit while mitigating the chance of critical overload during periods of worst-case weather conditions.

The key advantage of the NWP-based DTR system is the ability to provide a line rating based on the ampacity of the hottest span among all line spans. Other DTR systems overviewed in the current work provide ratings only for the spans where they are installed. Comparison of ampacities calculated for two relatively close (25 km apart) line spans (HOPE and AGASSIZ weather station locations) revealed a substantial difference in the average ampacities of the spans – 1202 A and 1502 A. This demonstrates that ambient weather conditions, particularly prevailing wind patterns, can be localized, changing ampacity significantly. If only some of the line spans are considered in DTR calculations, there is a risk that the actual hot spot of the line will be missed and the predicted rating will be higher than the actual line ampacity. The results of a case study demonstrated that the average line ampacity (983 A) calculated using a DTR-NWP approach was less than the average ampacities (1202 A and 1502 A) estimated for single line spans. Therefore, the NWP-based DTR is more reliable and safer than other DTR methods that calculate ratings for line spans only.

Although the DTR-NWP approach is preferred over other thermal rating methods, errors in ampacity calculations introduced through numerical weather

simulations can lead to violation of the thermal limit and line overheating. The accuracy of the WRF model (the NWP model used in the advanced DTR system) can be improved by a technique called model output statistics (MOS).

The research applies MOS to the DTR-NWP system and evaluates the improvement relative to untreated results. In a case study, MOS significantly reduced errors in predictions of ambient temperature, wind speed, and wind direction. The bias of the forecasted weather parameters was almost removed by MOS postprocessing. Reduction of MAE and RMSE was in the range of 20 % to 60 %, where the greater improvement was observed in the forecasts of wind speed.

Higher accuracy in numerical weather predictions leads to more accurate DTR calculations. Ampacity calculations performed for two different line spans based on the improved WRF data demonstrated a substantial reduction of errors in rating estimations. The risks of conductor overheating were also reduced when MOS were applied. The number of hours a conductor temperature exceeded 150 °C was reduced by 60 %.

To implement and efficiently utilize an NWP-based DTR system, modern information technologies must be applied. The quantity of weather data required to calculate accurate line ampacity depends on the temporal and spatial resolution of weather simulations and the length and number of transmission lines. As much data are required, efficient techniques of data manipulation and visualization are essential to the DTR system.

The research presents a database organization for the DTR system with the support of a geographical information system (GIS), numerical weather simulation, and actual weather measurements from remote climatological stations. Visualization techniques covered in the research include Web-based interactive graphics and plots and 3D visualization of transmission system assets. It is shown how advanced visualization methods and efficient data management of the DTR-NWP system can help a user make better decisions in a shorter time. Improved control

of the system would allow operators to plan maintenance and more realistically forecast energy demands.

The 3D visualization system, integrated with an energy management system (SCADA/EMS), can be used to visualize ampacities and energy flows in real time. Overlaid with weather maps, 3D representation of a transmission system will allow operators to monitor and control the condition of system assets in a more efficient and ergonomic way. From the training perspective, the 3D visualization system can be used for training of dispatchers. It can also provide more reliable and accurate support information for maintenance crews. Finally, the developed visualization system can be utilized as a user-friendly viewer of transmission systems. Utility employees will be able to explore the entire grid, virtually interact with the circuits, and examine their structural organization.

6.3 Future work

Future work on advanced weather-based thermal rating approaches will include: (i) in-depth analysis of the risks of line overheating associated with the chosen probabilistic ratings, (ii) improvement of MOS models and evaluation of MOS performance in areas different from those for which the MOS equations are built, (iii) analysis of the impact on MOS performance of low-wind speed errors in historical weather observations, and (iv) enhancement of software components of the advanced NWP-based DTR system.

Additional analysis of weather parameters and acceptable risk tolerance levels must be performed before applying probabilistic STRs (e.g., seasonal STR or STR based on TMY data) to everyday system operation. One way to mitigate thermal overload is to establish a correspondence between declared risks levels and actual risks, so that the final rating value must be selected based on risk values in a prepared lookup table. This will be attempted in future work.

The conducted research concludes that an advanced NWP-based DTR system improved with MOS and implemented with innovative information technologies is an effective and promising solution to the thermal rating of power transmission lines. The reliability of the DTR-NWP system depends on the accuracy of WRF weather predictions; therefore, a more thorough investigation of weather forecast errors must be performed. This will include comparison of NWP model results with historical weather observations recorded at various locations. Another possible improvement of the DTR-NWP system is to provide a confidence interval for each DTR calculation. In this case, a system operator will be able to make a decision based on a specified risk level (similar to probabilistic static thermal ratings). To build the DTR confidence intervals, uncertainties in the NWP simulations must be quantified.

Future research directions will also include further enhancements of the proposed database organization and data postprocessing algorithms. Several independent software tools that are currently used separately (DTR calculations, MOS, and database management) will be redesigned and integrated to assure efficient and reliable data flow. Web-based access to the system components will be also provided.

Finally, the development of the 3D visualization system will adapt a thin client approach, so that the application will reside on a server and be accessible to a user through a web-browser. By implementing the back-end logic on the server, it will be possible to avoid complexities of the system installation and configuration on the client machine. The future work on the 3D visualization system will also include development of a more robust graphical user interface and extension of program functionality to allow visualization of the future system states, based on weather forecasts.

Bibliography

[1] P. Musilek, "Advanced Dynamic Thermal Rating System Using Numerical Weather Prediction," Project Proposal 206099, 2009.

[2] International Energy Agency, "Environment Canada World Energy Outlook to 2010," tech. rep., 2010.

[3] D. Lawry and B. Fitzgerald, "Finding Hidden Capacity In Transmission Lines," North American Windpower, no. 3, 2007.

[4] D. A. Douglass, "Can Utilities Squeeze More Capacity Out of the Grid? Increased transmission circuit usage impacts risk and reliability.," Transmission and distribution world., vol. 55, no. 11, p. 38, 2003. ID: 98284897.

[5] R. Austria, "Upgrading Transmission Voltage - Planning Perspective," 2005.

[6] T. O. Seppa, "Reliability and real time transmission line ratings," tech. rep., The Valley Group A Nexans Company, 2007.

[7] M. W. Davis, "A new thermal rating approach: The real time thermal rating system for strategic overhead conductor transmission lines – Part I: General description and justification of the real time thermal rating system," Power Apparatus and Systems, IEEE Transactions on, vol. 96, no. 3, pp. 803–809, 1977. ID: 1.

[8] S. Cherukupalli, M. L. Lu, M. Siu, T. Macisaac, and K. Morison, "Field Trial of Dynamic Thermal Rating Devices on 230kV Indian Arm Crossing in British Columbia," in CIGRE Canada Conference on Power Systems, 2010.

[9] V. T. Morgan, "Rating of Bare Overhead Conductors for Continuous Currents," Proceedings of the Institution of Electrical Engineers-London, vol. 114, no. 10, p. 1473, 1967. PT: J; NR: 64; TC: 16; J9: PROC INST ELEC ENG; PG: 0; GA: A1399; UT: ISI:A1967A139900019.

[10] B. S. Howington and G. J. Ramon, "Dynamic Thermal Line Rating Summary and Status of the State-of-the-Art Technology," Power Delivery, IEEE Transactions on, vol. 2, no. 3, pp. 851–858, 1987. ID: 1.

[11] O. A. Ciniglio and A. K. Deb, "TRANSMISSION AND DISTRIBUTION - Optimizing Transmission Path Utilization in Idaho Power," IEEE transactions on power delivery : a publication of the Power Engineering Society., vol. 19, no. 2, p. 830, 2004. ID: 97168920.

[12] D. A. Douglass, D. C. Lawry, A. A. Edris, and E. C. B. III, "Dynamic thermal ratings realize circuit load limits," Computer Applications in Power, IEEE, vol. 13, no. 1, pp. 38–44, 2000. ID: 1.

[13] D. C. Lawry and J. R. Daconti, "Overhead line thermal rating calculation based on conductor replica method," in Transmission and Distribution Conference and Exposition, 2003 IEEE PES, vol. 3, pp. 880–885 vol.3, 2003. ID: 1.

[14] B. Forbes, D. Bradshaw, and F. Campbell, "Finding "Hidden Capacity" In Transmission Lines - Innovative device monitors sag and clearance enabling two utilities to increase power flow and defer line rebuilds.," Transmission & distribution world., vol. 54, no. 9, p. 30, 2002. ID: 96063381.

[15] T. O. Seppa, "Accurate ampacity determination: temperature-sag model for operational real time ratings," Power Delivery, IEEE Transactions on, vol. 10, no. 3, pp. 1460–1470, 1995. ID: 1.

[16] Arteche, "Temperature measurement sensor: SMT User Manual," 2008.

[17] G. M. Beers, S. R. Gilligan, H. W. Lis, and J. M. Schamberger, "Transmission Conductor Ratings," IEEE Transactions on Power Apparatus and Systems, vol. 82, no. 68, pp. 767–775, 1963. ID: 1.

[18] H. E. House and P. D. Tuttle, "Current-Carrying Capacity of ACSR," Power Apparatus and Systems, Part III. Transactions of the American Institute of Electrical Engineers, vol. 77, no. 3, pp. 1169–1173, 1958. ID: 1.

[19] D. Koval and R. Billinton, "Determination of Transmission Line Ampacities by Probability and Numerical Methods," IEEE Transactions on Power Apparatus and Systems, vol. PAS-89, no. 7, pp. 1485–1492, 1970. ID: 4639605996.

[20] M. W. Davis, "A New Thermal Rating Approach: The Real Thermal Rating System for Strategic Overhead Conductor Transmission Lines Part V Monthly and Annual Accumulative Frequency Distributions of Hourly Real-Time Thermal Rating and their Comparison with Conventional Rating-Risk Curves," Power Apparatus and Systems, IEEE Transactions on, vol. PAS-99, no. 6, pp. 2193–2209, 1980. ID: 1.

[21] M. W. Davis, "A new thermal rating approach: The real time thermal rating system for strategic overhead conductor transmission lines – Part II: Steady state thermal rating program," Power Apparatus and Systems, IEEE Transactions on, vol. 96, no. 3, pp. 810–825, 1977. ID: 1.

[22] M. W. Davis, "A New Thermal Rating Approach: The Real Time Thermal Rating System for Strategic Overhead Conductor Transmission Lines Part III Steady State Thermal Rating Program Continued-Solar Radiation Considerations," Power Apparatus and Systems, IEEE Transactions on, vol. PAS-97, no. 2, pp. 444–455, 1978. ID: 1.

[23] M. W. Davis, "A New Thermal Rating Approach: The Real Time Thermal Rating System for Strategic Overhead Conductor Transmission Lines Part IV Daily Comparisons of Real-Time and Conventional Thermal Rating and Establishment of Typical Annual Weather Models," Power Apparatus and Systems, IEEE Transactions on, vol. PAS-99, no. 6, pp. 2184–2192, 1980. ID: 1.

[24] W. Z. Black and W. R. Byrd, "Real-Time Ampacity Model for Overhead Lines," Power Apparatus and Systems, IEEE Transactions on, vol. PAS-102, no. 7, pp. 2289–2293, 1983. ID: 1.

[25] R. A. Bush, W. Z. Black, T. C. Champion, and W. R. Byrd, "Experimental Verification of a Real-Time Program for the Determination of Temperature and SAG of Overhead Lines," Power Apparatus and Systems, IEEE Transactions on, vol. PAS-102, no. 7, pp. 2284–2288, 1983. ID: 1.

[26] S. D. Foss, S. H. Lin, and R. A. Fernandes, "Dynamic Thermal Line Ratings Part I Dynamic Ampacity Rating Algorithm," Power Apparatus and Systems, IEEE Transactions on, vol. PAS-102, no. 6, pp. 1858–1864, 1983. ID: 1.

[27] S. D. Foss, S. H. Lin, H. R. Stillwell, and R. A. Fernandes, "Dynamic Thermal Line Ratings Part II Conductor Temperature Sensor and Laboratory Field test Evaluation," Power Apparatus and Systems, IEEE Transactions on, vol. PAS-102, no. 6, pp. 1865–1876, 1983. ID: 1.

[28] D. A. Douglass, "Weather-dependent versus static thermal line ratings (power overhead lines)," IEEE Transactions on Power Delivery, vol. 3, no. 2, pp. 742–753, 1988. ID: 4658375170.

[29] J. F. Hall and A. K. Deb, "Prediction of overhead transmission line ampacity by stochastic and deterministic models," Power Delivery, IEEE Transactions on, vol. 3, no. 2, pp. 789–800, 1988. ID: 1.

[30] P. M. Callahan and D. A. Douglass, "An experimental evaluation of a thermal line uprating by conductor temperature and weather monitoring," IEEE Transactions on Power Delivery, vol. 3, no. 4, pp. 1960–1967, 1988. ID: 1.

[31] J. W. Jerrell, W. Z. Black, and T. J. Parker, "Critical span analysis of overhead conductors," Power Delivery, IEEE Transactions on, vol. 3, no. 4, pp. 1942–1950, 1988. ID: 1.

[32] J. Ausen, B. F. Fitzgerald, E. A. Gust, D. C. Lawry, J. P. Lazar, and R. L. Oye, "Dynamic Thermal Rating System Relieves Transmission Constraint,"

in Transmission & Distribution Construction, Operation and Live-Line Maintenance, 2006. ESMO 2006. IEEE 11th International Conference on, 2006. ID: 1.

[33] M. M. Saied, "Assessing the dynamic rating of overhead transmission lines," EUROPEAN TRANSACTIONS ON ELECTRICAL POWER, vol. 17, no. 5, pp. 526–536, 2007. ID: 211757498.

[34] J. R. Harvey, "Effect of Elevated Temperature Operation on the Strength of Aluminum Conductors," Power Apparatus and Systems, IEEE Transactions on, vol. PAS-91, no. 5, pp. 1769–1772, 1972. ID: 1.

[35] IEEE Power Engineering Society, "IEEE Standard for Calculating the Current-Temperature of Bare Overhead Conductors," 2007. ID: 1.

[36] L. M.L. and K. Z., "Accuracy of transmission line modeling based on aerial LiDAR survey," IEEE Trans Power Delivery IEEE Transactions on Power Delivery, vol. 23, no. 3, pp. 1655–1663, 2008. ID: 280728740.

[37] H. Wan, J. D. McCalley, and V. Vittal, "Increasing thermal rating by risk analysis," IEEE Transactions on Power Systems, vol. 14, no. 3, pp. 815–828, 1999. ID: 1.

[38] CIGRE, "Thermal Bahavior of Overhead Conductors," Electra, no. 144, 1992.

[39] N. P. Schmidt, "Comparison between IEEE and CIGRE ampacity standards," IEEE Transactions on Power Delivery, vol. 14, no. 4, pp. 1555–1559, 1999. ID: 1.

[40] P. Zhang, M. Shao, A. R. Leoni, D. H. Ramsay, and M. Graham, "Determination of static thermal conductor rating using statistical analysis method," in Electric Utility Deregulation and Restructuring and Power Technologies, 2008. DRPT 2008. Third International Conference on, pp. 1237–1243, 2008. ID: 1.

[41] F. Mesinger, G. DiMego, E. Kalnay, K. Mitchell, P. C. Shafran, W. Ebisuzaki, D. Jovi, J. Woollen, E. Rogers, E. H. Berbery, M. B. Ek, Y. Fan, R. Grumbine, W. Higgins, H. Li, Y. Lin, G. Manikin, D. Parrish, and W. Shi, "North American Regional Reanalysis," Bulletin of the American Meteorological Society, vol. 87, no. 3, pp. 343–360, 2006. ID: 437790933.

[42] J. D. Glover and M. S. Sarma, Power system analysis and design. Boston: PWS Pub., 1994. ID: 28844159.

[43] F. R. McElvain and S. S. Mulnix, "Statistically determined static thermal ratings of overhead high voltage transmission lines in the Rocky Mountain region," IEEE Transactions on Power Systems, vol. 15, no. 2, pp. 899–902, 2000. ID: 1.

[44] J. Heckenbergerova, P. Musilek, and K. Filimonenkov, "Assessment of Seasonal Static Thermal Ratings of Overhead Transmission Conductors," in IEEE Power & Energy Society General Meeting, 2011.

[45] S. Wilcox, W. Marion, and N. R. E. L. (U.S.), Users manual for TMY3 data sets. Golden, CO: National Renewable Energy Laboratory, 2007. ID: 228111791.

[46] N. L. Inc, "Canadian weather for energy calculations (cwec) weather files."

[47] D. A. Douglass, "Uprating Transmission Lines and Reducing Risk: Incremental uprating methods can be used to increase thermal line ratings," Transmission & distribution world, March 1998.

[48] D. S. Wilks, Statistical methods in the atmospheric sciences. Burlington, MA; London: Academic Press, 2006. ID: 62345198.

[49] H. R. Glahn and D. A. Lowry, "The Use of ModelOutputStatistics (MOS) in ObjectiveWeatherForecasting," Journal of Applied Meteorology, vol. 11, no. 8, pp. 1203–1211, 1972.

[50] J. C. Maloney, "ETA-BASED MOS PROBABILITY OF PRECIPTATION AMOUNT GUIDANCE FOR THE CONTINENTAL UNITED STATES," CONFERENCE ON WEATHER ANALYSIS AND FORECASTING, vol. 19, pp. 415–418, 2002. ID: 202774580.

[51] L. A. Vincent, W. Wijngaarden, and R. Hopkinson, "Surface Temperature and Humidity Trends in Canada for 1953-2005," Journal of Climate, no. 20, pp. 5100–5113, 2007.

[52] E. Canada, "Climate Data Online," 2011.

[53] J. P. Thompson, "Web-based enterprise management architecture," IEEE Communications Magazine, vol. 36, no. 3, pp. 80–86, 1998.

[54] L. Grasberg and L. Osterlund, "SCADA EMS DMS–A Part of the Corporate IT System," in PROCEEDINGS OF THE INTERNATIONAL CONFERENCE ON POWER INDUSTRY COMPUTER APPLICATIONS, pp. 141–147, 2001.

[55] R. Blum, PostgreSQL 8 for Windows. New York: McGraw-Hill, 2007.

[56] S. Steiniger and E. Bocher, "An overview on current free and open source desktop GIS developments," International Journal of Geographical Information Science, vol. 23, no. 10, pp. 1345–1370, 2009.

[57] E. V. der Vlist, D. Ayers, and E. Bruchez, Professional Web 2.0 programming. Indianapolis, IN: Wrox/Wiley, 2007.

Appendix A

MOS predictors and coefficients

Predictor	Height	Description
q2wrf	2 m	water vapor mixing ratio at 2 m
t2wrf	2 m	ambient temperature at 2 m
u10wrf	10 m	x-wind component
v10wrf	10 m	y-wind component
wspd10wrf	10 m	wind speed at 2 m
pslwrf	2 m	sea level pressure
psfcwrf	2 m	surface pressure
rh2wrf	2 m	relative humidity at 2 m
td2wrf	2 m	dew temperature at 2 m
Predictor	Pressure levels	Description
t950, t925, t850, t700, t500	950 mb 925 mb 850 mb 700 mb 500 mb	ambient temperature at corresponding pressure levels
w950, w925, w850, w700, w500		z-wind component at corresponding pressure levels
u950, u925, u850, u700, u500		x-wind component at corresponding pressure levels
v950, v925, v850, v700, v500		y-wind component at corresponding pressure levels
wspd950, wspd925, wspd850, wspd700, wspd500		wind speed at corresponding pressure levels

Table A.1: Predictors (WRF variables) used for building MOS models.

Station name	Season	MOS coefficients (ambient temperature model)				
		(Intercept)	t2wrf	wspd10wrf	u10wrf	v10wrf
AGASSIZ	winter	-36.703	0.418	0.070	-0.172	0.039
AGASSIZ	summer	-29.358	0.826	-0.112	-0.090	0.039
HOPE	winter	-76.898	0.484	-0.081	0.115	0.054
HOPE	summer	-34.420	0.675	-0.101	0.134	0.033
		psfcwrf	pslwrf	rh2wrf	td2wrf	q2wrf
AGASSIZ	winter	0.000			0.291	-477.341
AGASSIZ	summer	-0.071	0.070	0.079	-0.340	301.194
HOPE	winter	-0.005	0.006	0.058	0.084	-320.450
HOPE	summer	-0.059	0.058	0.102	-0.190	
		w950	w925	w850	w700	w500
AGASSIZ	winter	0.307			0.196	
AGASSIZ	summer	-0.995	0.743	-0.339		-0.148
HOPE	winter		-0.231	0.121	-0.134	
HOPE	summer	-0.853	0.729	-0.184	-0.263	-0.186
		t950	t925	t850	t700	t500
AGASSIZ	winter	0.614	0.152	-0.372	-0.077	0.060
AGASSIZ	summer	0.381		0.147	-0.116	0.101
HOPE	winter	1.409	-0.363	-0.509	-0.097	0.064
HOPE	summer	0.994		-0.390	0.084	
		u950	u925	u850	u700	u500
AGASSIZ	winter	0.162		-0.023	-0.145	0.050
AGASSIZ	summer	0.151	-0.185			0.032
HOPE	winter	-0.136	0.149		-0.087	0.026
HOPE	summer		0.155	-0.042	0.026	0.039
		v950	v925	v850	v700	v500
AGASSIZ	winter		-0.074	-0.020	-0.030	
AGASSIZ	summer	0.151	-0.102		-0.021	0.013
HOPE	winter			-0.125	-0.027	
HOPE	summer	-0.167	-0.158	-0.087	0.023	-0.012
		wspd950	wspd925	wspd850	wspd700	wspd500
AGASSIZ	winter		0.063	-0.029	0.062	-0.054
AGASSIZ	summer	-0.043	0.088	-0.075	-0.029	-0.025
HOPE	winter	-0.129	0.163	0.074		-0.036
HOPE	summer	-0.221	0.142		-0.054	-0.022

Table A.2: MOS coefficients for the model of ambient temperature.

Station name	Season	MOS coefficients (wind speed model)				
		(Intercept)	t2wrf	wspd10wrf	u10wrf	v10wrf
AGASSIZ	winter	12.880	-0.029	0.127	0.064	0.060
AGASSIZ	summer	-9.947	0.017	0.185		0.033
HOPE	winter	15.134		0.210	-0.074	0.035
HOPE	summer	2.070	0.058	0.156	0.044	0.084
		w950	w925	w850	w700	w500
AGASSIZ	winter		0.262		0.123	
AGASSIZ	summer	0.241		0.103		-0.096
HOPE	winter	0.898	-0.300	-0.168		-0.096
HOPE	summer	0.627	-0.597	0.340	-0.112	
		t950	t925	t850	t700	t500
AGASSIZ	winter	-0.399	0.351	0.048		-0.019
AGASSIZ	summer	0.017		0.021	-0.027	-0.026
HOPE	winter	0.539	-0.871	0.310	-0.034	
HOPE	summer	-0.120		0.101		-0.013
		u950	u925	u850	u700	u500
AGASSIZ	winter	-0.100	0.050	-0.067		-0.019
AGASSIZ	summer	-0.063		-0.050	0.011	-0.005
HOPE	winter	-0.066		-0.017	0.040	
HOPE	summer	-0.087			0.060	
		v950	v925	v850	v700	v500
AGASSIZ	winter		-0.047	-0.033	0.036	-0.024
AGASSIZ	summer				0.018	-0.010
HOPE	winter	-0.122	0.073	-0.019	0.032	
HOPE	summer			-0.016	0.042	
		wspd950	wspd925	wspd850	wspd700	wspd500
AGASSIZ	winter	0.119	-0.048	0.056		0.031
AGASSIZ	summer	0.058	0.014		-0.028	0.011
HOPE	winter	0.112	0.058		-0.014	0.016
HOPE	summer	0.078	0.032		-0.062	0.006
		psfcwrf	pslwrf			
AGASSIZ	winter		0.000			
AGASSIZ	summer		0.000			
HOPE	winter	0.002	-0.002			
HOPE	summer					

Table A.3: MOS coefficients for the model of wind speed.

Station name	Season	MOS coefficients (wind direction model)				
		(Intercept)	u10wrf	v10wrf		
AGASSIZ	winter	39.779	-0.765	0.436		
AGASSIZ	summer	38.857				
HOPE	winter	68.593	-0.286	0.313		
HOPE	summer	69.169		0.524		
		w950	w925	w850	w700	w500
AGASSIZ	winter	2.565		-1.181		
AGASSIZ	summer	2.589			2.755	
HOPE	winter				-0.774	-0.867
HOPE	summer		-3.122	2.061		
		u950	u925	u850	u700	u500
AGASSIZ	winter		-0.299	0.516	-0.293	0.118
AGASSIZ	summer	0.712	-0.496		0.144	-0.080
HOPE	winter		-0.287	-0.158	0.091	
HOPE	summer		-0.611	-0.375	0.149	
		v950	v925	v850	v700	v500
AGASSIZ	winter	0.468		0.317	-0.201	
AGASSIZ	summer		0.505			0.057
HOPE	winter	0.493		-0.269	0.293	
HOPE	summer	0.421	0.720	-0.385	0.102	

Table A.4: MOS coefficients for the model of wind direction.